

Experimental Studies on Xonotlite in the $\text{SiO}_2\text{-CaO-H}_2\text{O}$ System —With Special Reference to the Spherical Secondary Particles—

By

KAZUO SHIBAHARA

With 8 Tables, 3 Text-figures and 7 Plates

(Received, January 26, 1987)

ABSTRACT

Synthetic xonotlite is one of the most important constituents of the industrial material for heat insulating and fire-resistant building materials. In this paper, formation mechanism of xonotlite as well as spherical secondary particle were experimentally examined in the $\text{SiO}_2\text{-CaO-H}_2\text{O}$ system. Special attention was paid for the process of crystal growth and effects of the crystalline state of the starting materials. Effects of Al_2O_3 in the starting materials were also investigated using both pure and industrial materials. The products obtained were examined by X-ray diffraction and electron diffraction in addition to the detailed observations under the stereoscope and electron microscope. Amorphous to semi-crystalline state of C-S-H was characteristically formed at the initial stage of reaction and the morphology and the crystalline state of C-S-H varied complicatedly according to the experimental conditions.

The main results obtained are as follows: Morphology of C-S-H and its aggregate depend largely upon the crystalline state of the starting materials. In the experiments used Brazilian quartz as source of silica, fine and fibrous C-S-H is aggregated, forming angular surfaced massive agglomerate. Using silica gel (reagent), fine aggregate particle of crumpled foil of C-S-H is entangled with long and fibrous C-S-H, resulting in an irregular massive agglomerate. Most of C-S-H formed in the Brazilian quartz system transform to platy tobermorite and to strip and needle crystals of xonotlite through platy tobermorite as reaction proceeds, and simultaneously massive agglomerate of slightly rounded form changes to oolitic (A_1) and spherical-shelled (A_2) secondary particles. The formation process of the spherical secondary particle composed of xonotlite is basically the same as that when industrial silica powder (α -quartz) containing a very small quantity of Al_2O_3 is used. With increasing particle size of CaO, hollow spherical secondary particles change to those of dense aggregates composed of needle crystals of xonotlite (A_3) through the spherical shell (A_2) and oolitic (A_1).

In the experiments used silica gel (reagent), C-S-H transforms directly to needle crystal of xonotlite which aggregates in the forms of bundle or irregular massive agglomerate, and no spherical agglomerate is formed. With rising temperatures, however, prisms of hillebrandite are partly formed and transform to xonotlite, forming the spherical secondary particle (B_1) composed of extremely coarse aggregates with long needle xonotlite on the surface. By addition of very small amount of Al_2O_3 , spherical secondary particles are formed in such a way that long fibrous C-S-H formed at the initial stage of the reaction becomes gradually short resulting the number of bundled aggregates decrease and then, as the reaction proceeds, the platy crystal of tobermorite is partly formed which later transforms into xonotlite forming spherical secondary particles. The secondary particle is composed of relatively coarse aggregates of needle crystals (B_2). The spherical secondary particle is unevenly hollow and has long needle crystals on the surface. To be noted is that the texture and morphology of these spherical secondary particles are similar to those produced in the industrial processes when byproduct amorphous silica containing a very small quantity of Al_2O_3 is used.

The spherical secondary particle of types A_1 , A_2 , B_1 and B_2 play an important role producing light-weighted products suited for insulation and heat insulating materials and that of A_3 is suited for fire-resistant building materials because of the high density property. Aggregates composed of the needle crystals of xonotlite do not form the secondary particle and the products have drawbacks such as poor mouldability and contraction and distortion during the drying. These aggregates could not be used as the industrial materials.

CONTENTS

- I. Introduction
- II. Experimental method
 - A. Starting material
 - B. Synthetic method
- III. Experimental results
 - A. X-ray powder diffraction
 - B. Rate of crystal growth
 - C. Lattice constants
 - D. Selected area electron diffraction and transmission electron microscopic observations
 - E. Specific surface area and ignition loss

- IV. Morphology and texture, and its relationships to the industrial products
- V. Formation mechanism of the spherical secondary particle
- VI. Summary
- References

I. INTRODUCTION

Although synthetic xonotlite is widely used as the industrial materials such as thermal insulators and fire-resistant building materials, natural occurrence of the mineral is relatively rare. Since the first discovery of xonotlite by Rammelsberg (1866), several natural occurrences of the mineral have been reported (Larsen, 1917; Eakle, 1921; Shannon, 1925; Berman, 1937; Ohmori, 1939 and Imai et al., 1972).

As the ideal chemical formula of xonotlite, a formula of $\text{Ca}_3(\text{Si}_3\text{O}_8)(\text{OH})_2$ was proposed by Berman (1937). Later, Mamedov et al. (1955), re-examined the mineral and $\text{Ca}_6(\text{Si}_6\text{O}_{17})(\text{OH})_2$ was obtained based on their precise measurements of the cell dimensions and density. Natural xonotlite, however, commonly contains a small amount of impurities such as Al, Mg and Fe.

Synthesis of xonotlite was first reported by Nagai (1931a, b and 1933). Xonotlite is easily formed over wide temperature and pressure range in the $\text{CaO-SiO}_2\text{-H}_2\text{O}$ system, which is one of the most important systems in the fields of cement and/or ceramics, and many synthetic experiments have been performed up to the present (Flint et al., 1938; Heller et al., 1951; Peppler, 1955; Akaiwa et al., 1956; Assarsson, 1957 and 1958; Aitken et al., 1960; Speakman, 1968; Takahashi et al., 1972b and 1973; Kalousek et al., 1977; Chan et al., 1978; Ishii et al., 1978 and others).

As the results of these investigations, industrial production methods have been established, i.e., filter press moulding, pan casting moulding and active slurry methods (Kubo, 1980 and Mitsuda, 1980). Among these, the active slurry method is used most commonly and is employed in the present experiment. According to Kubo et al. (1974a, b, c and 1980) and Ciach et al. (1980), the reaction process of active slurry method is briefly explained as follows: reaction of $\text{SiO}_2\text{-CaO-H}_2\text{O}$ system is carried out under stirring hydrothermal conditions; the crystals of calcium silicate hydrate are aggregated forming spherical secondary particles of 5 to 150 μm in diameter in the form of slurry; and the final product is obtained by moulding and drying the slurry; thus the particles of the product contact and entangle with each other resulting in intense strength. The method is, in other words, basically to produce the spherical secondary particles of the crystals of calcium silicate hydrate.

It is to be noted that the physical properties of the final product such as density and strength largely depend upon the texture and morphology of spherical secondary particle of xonotlite, especially upon the degree of roundness of the secondary particles. When the secondary particle is not spherical, the product shows drawbacks such as contraction and distortion during the drying. It is, therefore, very important to control the formation of spherical secondary particle in the active slurry method.

However, systematic examinations on the formation mechanisms of the spherical secondary particles have not

been carried out up to the present. Kubo et al. (1974b and 1978) reported preliminary experimental results concerning the secondary particles but their starting materials were industrial ones containing much impurities. The main purpose of this paper is to present fundamental data on the crystal growth in the reaction system using pure reagents and on the formation mechanism of the secondary particles. Special attention was paid to the effects of the starting materials, especially to the role of Al_2O_3 , reaction temperature and time in relation to the crystal growth, and furthermore to the formation process of spherical secondary particle. The results obtained were also discussed in comparison with the previous experimental results concerning the industrial materials (Shibahara et al., 1986a and b).

Acknowledgments

The author wishes to express his sincerest gratitude to Professor Satoru KAKITANI of the Hiroshima University for his constant and invaluable advice rendered during the course of the work as well as for his critical reading of the manuscript. The author is also indebted to Professors Akira SOEDA and Ikuo HARA and Associate Professor Yuji OKIMURA of the same University for their guidance and critical advice. He also gratefully acknowledges his debt to Associate Professor Setsuo TAKENO of the same University for his discussions and for critical reading of the manuscript. He is also indebted to Associate Professor Hiroshi YAMAGUCHI of the Osaka Kyoiku University and Associate Professor Tadaomi KOHNO of the Kyushu Industrial University for their stimulating and helpful discussions. Thanks are also due to Dr. Ryuji KITAGAWA, Dr. M. SUZUKI, Dr. T. SHIMAMOTO and Dr. T. MIYAMOTO of the Hiroshima University for their helpful advice and encouragement.

He is also indebted to Professor Mitsue KOIZUMI of the Osaka University for his constant and valuable advice and encouragement.

Special thanks are also due to Mr. Katsumi KAKIGI, Osaka Packing Manufacturing Co., Ltd., President, for providing the opportunity of the present study and permitting the presentation of the report. Thanks are also due to Mr. Kazuhiko KUBO, Chief of Production Division, Mr. Akira TAKAHASHI, Chief of Technical Research Department and Mr. Tatsuya MINOURA, Deputy Chief of Technical Research Department, for their assistance and cooperation in the work. His thanks are also to be expressed for the use of the electron diffraction afforded by Professor Yasutaka TAKAHASHI of the Gifu University, and Mr. Hideo HAYASHI of the Government Industrial Research Institute, Osaka.

II. EXPERIMENTAL METHOD

A. STARTING MATERIAL

1. SILICA (SiO₂)

In the present experiment, pure Brazilian quartz pulverized to about 6.4 μm in size was used. The size of the starting material was determined considering the fact that above 30 μm , no spherical secondary particles were producible. Special reagent silica gel with average size of 5.7 μm was also used in order to examine the effects of the crystalline state of starting materials.

For comparative study, industrial materials were also used, i.e., one is natural silicestone (α -quartz) from Tajimi City, Gifu Prefecture, with the average size of 7.3 μm and by-product silica powder (amorphous) with size of about 0.33 μm . Chemical compositions of these starting materials are shown in Table 1.

TABLE 1. CHEMICAL COMPOSITION OF THE STARTING MATERIAL OF SILICA.

Starting material	SiO ₂	Al ₂ O ₃	Fe ₂ O ₃	MgO	Ig. loss
Brazilian quartz	99.58	0.03	0.02	tr.	0.26
Silica gel (reagent)	94.66	0.05	0.03	tr.	4.90
Silica powder (1)	97.87	0.99	0.49	0.12	0.31
By-product silica (2)	95.20	0.71	0.07	0.06	2.48

(1): After Shibahara et al. (1986 b).

(2): After Shibahara et al. (1986 a).

2. LIME (CaO)

Special reagent calcium carbonate calcined at 1000°C for ten hours and natural limestone from Akasaka, Gifu Prefecture, calcined at temperatures of 1000, 1100 and 1200°C for four hours were used. It was confirmed by X-ray powder diffraction method that no uncalcined calcite was present in these samples. The three calcination temperatures were chosen to examine the effect of the heating temperature. The particle size of the pure and the industrial limes calcined at 1000°C is almost equal with each other and the size increases with raising calcining temperature. The relationship between the calcining temperature and the crystalline particle size agrees with those of Ohno et al. (1957) and Sakaeda et al. (1969).

The chemical compositions and the particle size determined by the scanning electron microscope are shown in Table 2.

TABLE 2. CHEMICAL COMPOSITION AND PARTICLE SIZE OF THE STARTING MATERIAL OF LIME.

Starting material	CaO	Al ₂ O ₃	MgO	Ig. loss	Particle size of CaO
Pure lime (prepared by calcining reagent calcium carbonate at 1000° C for 10 h)	99.74	0.06	0.13	0.07	0.3 to 1.0 μm
Industrial lime (prepared by calcining limestone at 1000° C for 4 h) (1)	96.25	—	—	0.23	0.5 to 1.2 μm
Industrial lime (prepared by calcining limestone at 1100° C for 4 h) (2)	97.27	0.13	0.74	0.21	—
Industrial lime (prepared by calcining limestone at 1100° C for 4 h) (3)	96.95	—	—	0.16	0.8 to 2.2 μm
Industrial lime (prepared by calcining limestone at 1200° C for 4 h) (4)	96.96	—	—	0.16	CaO crystals were sintered

(1), (3) and (4): Data were taken from Shibahara et al. (1986 b) (Limestone composed of 54.43% of CaO, 0.32% of MgO, 0.05% of Fe₂O₃, 0.09% of Al₂O₃, 0.13% of SiO₂ and 44.98% of ignition loss was used).

(2): After Shibahara et al. (1986 a).

3. Al₂O₃

γ -Al₂O₃ of special grade reagent of 99.8% purity

with average size of 0.02 μm and natural clay composed of mainly kaolin minerals (46.63%, SiO₂; 35.23%, Al₂O₃; 2.41%, Fe₂O₃; 0.71%, MgO and 13.10% of ignition loss) from Ohita Prefecture were used as the starting material of aluminum.

B. SYNTHETIC METHOD

In the case of pure materials, special grade of reagents were precisely weighed so that the atomic ratio of Ca/Si was equal to the stoichiometric ratio in xonotlite, i.e., 1.00, and that of Al/Si was to 0.025 for the aluminum containing case. Thus, the starting compound contains 1.05 wt. % of Al₂O₃. Amount of Al₂O₃ was decided considering the aluminum content of the industrial raw material or the chemical composition of natural xonotlite. This is because xonotlite is not produced under the ordinary industrial conditions of temperature and pressure when the addition of Al₂O₃ exceeds approximately 2 wt. % (Takahashi et al., 1973).

Twelve times distilled water of 85°C by weight was added to the starting lime to slake it. Silica and Al₂O₃ were added to the solution under stirring. Then, distilled water was further added to obtain 2 ℓ of slurry in which the weight ratio of water/starting material was 20. The slurry was put into an autoclave (I.D.: 13 cm, 3 ℓ Volume) equipped with the agitator and was heated under the rotating condition of the agitator at 100 rpm. The heating rate was controlled so that it reached 175°C (8 kg/cm²), 191°C (12 kg/cm²) or 214°C (20 kg/cm²) from 100°C in one hour. Under these conditions, reaction was continued for 1, 2, 4, 6, 8, 12, 24, and 48 hours and 7 days. The content was stirred for 24 hours in the 7 day's run.

In case of experiments using the industrial starting materials, the atomic ratio of Ca/Si was controlled to be 0.975 according to the experimental result of Kubo et al. (1974a, b, 1976 and 1978), and the weight ratios of water/starting material were fixed 12 and 20 for silica powder (α -quartz) and amorphous by-product silica, respectively. The hydrothermal reaction was performed at 191°C (12 kg/cm²) for eight hours. The other conditions were the same as those for the pure material.

After it was held for certain hours at a known temperature, the autoclave was cooled by cutting electricity, and the product was taken out. The temperature range of the reaction between 175°C (8 kg/cm²) and 214°C (20 kg/cm²) was decided with reference to the conditions applied usually to the industrial processes.

III. EXPERIMENTAL RESULTS

A. X-RAY POWDER DIFFRACTION

After experimental products were dried at 100°C for twenty four hours, their X-ray powder patterns were taken to identify the mineral constituent. To examine the growth process of xonotlite, the conditions of X-ray diffraction were kept constant as follows: X-ray: CuK α , with Ni-filter, 35 KV, 25 mA, receiving slit: 0.15 mm, divergent slit: 1°, time constant: 1 sec, scanning speed: 0.5°/min, rotating speed of chart: 10 mm/min. Amorphous to semi-crystalline state of calcium silicate hydrates are generally produced at the initial stage of the hyd-

rothermal reaction in the $\text{SiO}_2\text{-CaO-H}_2\text{O}$ system. Among them, the hydrate showing only the diffraction lines corresponding to (h k 0) and (0 0 l) is referred to C-S-H according to Taylor (1964).

The results are summarized in Table 3. Some typical results showing phase change with duration of the reaction time are shown in Figs. 1, 2 and 3. The detailed phase change of the respective starting materials will be briefly described in the following.

TABLE 3. MINERALOGICAL CONSTITUENTS OF THE EXPERIMENTAL PRODUCTS.

Starting material of SiO_2	Starting material of Al_2O_3	Reaction condition			Products
		Temp.(°C)	Press.(kg/cm ²)	Time(h)	
Brazilian quartz	—	191	12	2	C
				4	T, X, C*
				6	X, T
				8	X, T
				24	X
				168	X
Silica gel (reagent)	—	175	8	12	C
				24	X
				48	X
		191	12	2	C
				4	C
				6	C, H*
				8	X, C*
				24	X
				168	X
		214	20	1	C
				2	C, H
				4	X
Silica gel (reagent)	$\gamma\text{-Al}_2\text{O}_3$	191	12	8	C, T*
				12	C, T*
				24	X, C*
				168	X
	Kaolin	191	12	8	C, T*
				12	X, C*
				24	X, C*
				168	X

* Only several main reflections were observed.

1. In the reaction of Brazilian quartz (SiO_2)-CaO- H_2O system at 191°C (12 kg/cm²), a very weak reflection of (002) of C-S-H at about 11.3 Å (2θ : 7.8) can be recognizable in addition to the broad peaks of (220) and (040) near $d=3.1$ Å (2θ : 29) and $d=1.84$ Å (2θ : 49.5), respectively, after two hours reaction. As is seen in Fig. 1, some unreacted α -quartz still remains in the system. After four hours, however, only a little amount of α -quartz remains, while tobermorite and xonotlite begin to appear. In six hours, α -quartz reacts almost completely, while amount of xonotlite increases. In eight hours, xonotlite becomes predominant. In twenty four hours, tobermorite is hardly observed, and the whole product is composed of xonotlite as shown in Fig. 1. In such a way, xonotlite is produced from the amorphous material through tobermorite and the spherical secondary particle is formed.

2. In the reaction of silica gel (reagent SiO_2)-CaO- H_2O system, no spherical secondary particles were produced at 191°C (12 kg/cm²). Therefore, reactions at

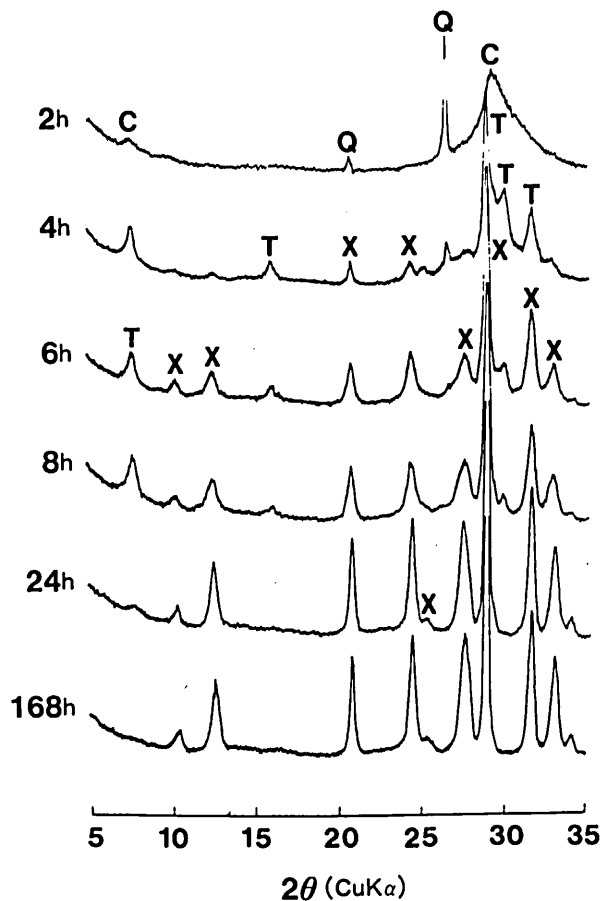


FIG. 1. X-ray diffraction patterns of the products in Brazilian quartz-CaO- H_2O system. Reaction conditions: 191°C (12 kg/cm²); 2, 4, 6, 8, 24 and 168 h, respectively. C: C-S-H, H: Hillebrandite, T: Tobermorite, X: Xonotlite, Q: α -quartz

175°C (8 kg/cm²) and 214°C (20 kg/cm²) were also investigated. In the reaction at 175°C (8 kg/cm²), C-S-H begins to appear after twelve hours. However, (400) reflection at about 2.82 Å (2θ : 31.7) is hardly observable in contrast with distinct reflections of (002), (220) and (040). After 24 hours, xonotlite becomes a predominant phase as shown in Fig. 2A, but no spherical secondary particles are formed. In the reaction at 191°C (12 kg/cm²), only C-S-H is recognized as in the reaction at 175°C after two and four hours. After six hours, however, reaction proceeds and a small and broad peak of a new phase begins to appear near $d=2.94$ Å (2θ : 30.4) in addition to C-S-H as is shown in Fig. 2B. Although the identification of the new phase is difficult due to weak diffraction peaks, the characteristic d-value may correspond to that of hillebrandite, $\text{Ca}_2(\text{SiO}_3)(\text{OH})_2$. After eight hours, the new phase disappears and the reflections of xonotlite are observable. Over eight hours, intensities of xonotlite reflections increase gradually, but no spherical secondary particles are formed. In the reaction at 214°C (20 kg/cm²), C-S-H is formed only after one hour. In two hours, broad peaks at $d=4.80$ Å (θ : 18.5), 3.55 Å (2θ : 25.1), 3.35 Å (2θ : 26.6), 3.05 Å (2θ : 29.3), 2.784 Å (2θ : 32.1) and $d=1.831$ Å (2θ : 49.8) in addition to the broad peak of $d=2.94$ Å (2θ : 30.4) are observable, the same as that observed in six hours in the

reaction at 191°C . These peaks indicate existence of hillebrandite besides C-S-H as are shown in Fig. 2C. In four hours, reflections of hillebrandite disappear and those of xonotlite appear, and furthermore, the spherical secondary particles are formed.

In conclusion, formation of hillebrandite from amorphous materials depends upon the reaction temperature.

3. In the experiments added $\gamma\text{-Al}_2\text{O}_3$ to the reaction system of silicagel (reagent SiO_2)- CaO - H_2O at 191°C (12 kg/cm^2), C-S-H is formed in runs of eight and twelve hours the same as that without Al_2O_3 . In runs of

twelve hours, another weak and broad peaks are clearly observed near $d=5.45\text{ \AA}$ ($2\theta: 16.3$), 3.55 \AA ($2\theta: 25.1$) and 1.672 \AA ($2\theta: 54.9$) as are shown in Fig. 3A. These reflections may probably be ascribed to those of tobermorite. After 24 hours, reflections of xonotlite become predominant and the spherical secondary particles are formed. By adding the clays containing kaolin minerals, some tobermorite as well as C-S-H are formed in eight hours. After twelve hours, xonotlite begins to appear as is shown in Fig. 3B. In the runs of 24 and 168 hours, reflections of xonotlite become more conspicuous and the

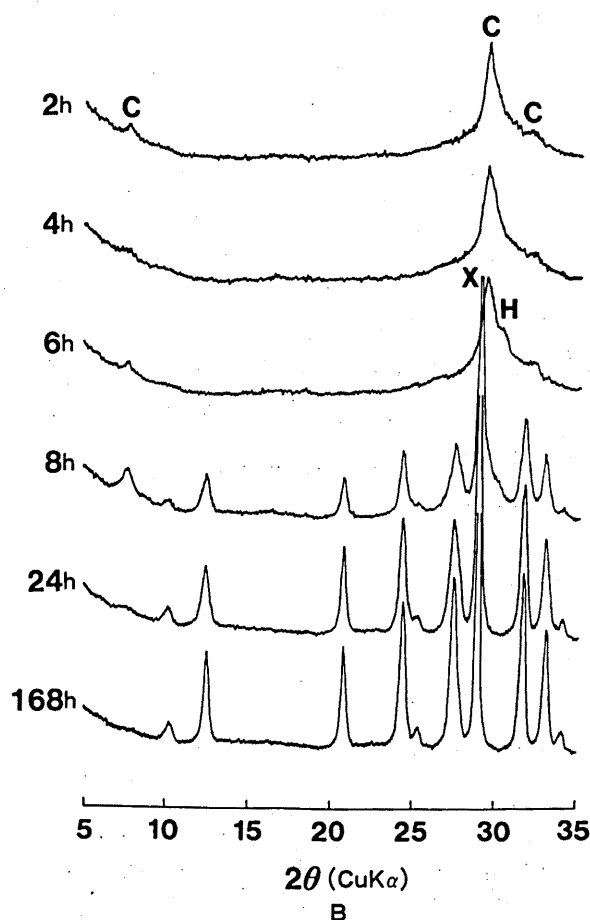
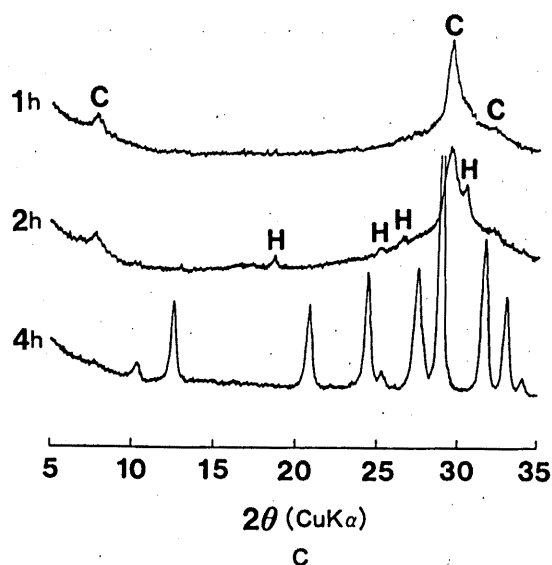
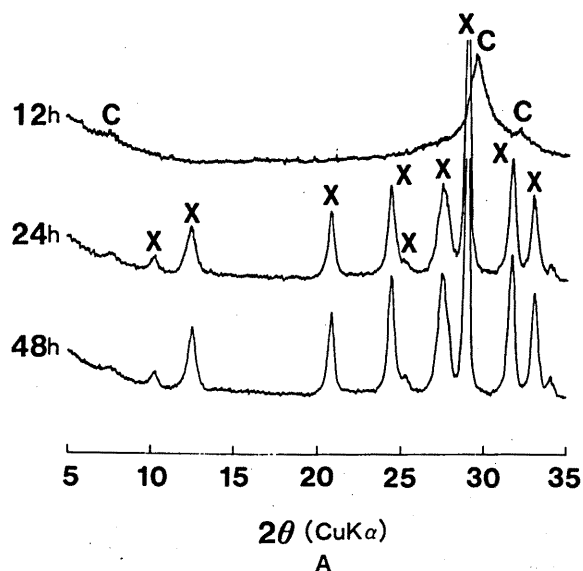


Fig. 2. X-ray diffraction patterns of the products in silica gel (reagent)- CaO - H_2O system.

A: 175°C (8 kg/cm^2); 12, 24 and 48 h, B: 191°C (12 kg/cm^2); 2, 4, 6, 8, 24 and 168 h, C: 214°C (20 kg/cm^2); 1, 2 and 4 h.

Abbreviations are the same as those of Fig. 1.

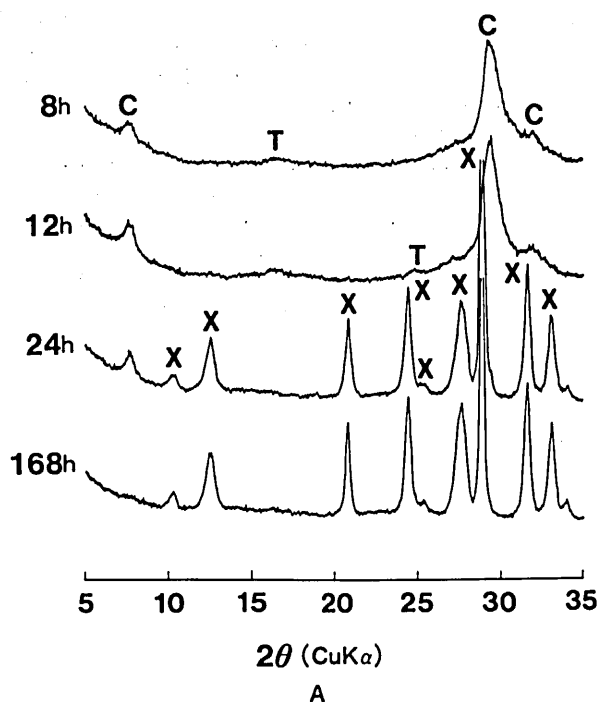
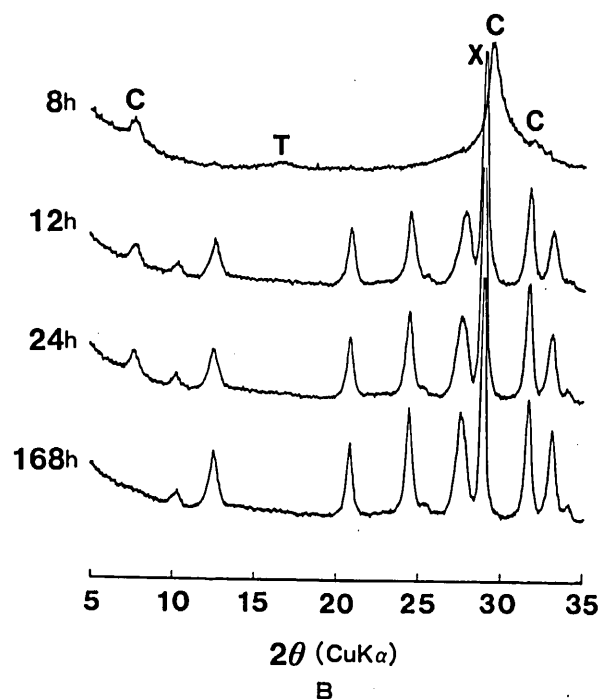


FIG. 3. X-ray diffraction patterns of the products in silica gel (reagent)-CaO-Al₂O₃-H₂O system. Reaction conditions: 191°C (12 kg/cm²); 8, 12, 24 and 168 h, respectively. A: Addition of γ -Al₂O₃, B: Addition of kaolin. Abbreviations are the same as those of Figs. 1 and 2.



spherical secondary particles are formed.

It may be concluded that the addition of Al₂O₃ retards the formation of xonotlite. That is, addition of γ -Al₂O₃ and that of kaolin prolong the reaction time of the first appearance of xonotlite approximately 3 times for the case of γ -Al₂O₃ and 1.5 times for kaolin, respectively, compared with that of the experiments without Al₂O₃.

B. RATE OF CRYSTAL GROWTH

The rate of crystal growth was investigated by measuring the intensity of X-ray diffraction. Assuming that the diffraction intensity (height of peak) of $d=3.64$ Å (401) of xonotlite formed in reaction at 191°C (12 kg/cm²) for seven days using silica gel (reagent) is 100, relative intensity of (401) was measured for all xonotlite and the value is supposed to represent the crystallization state. The reason why the peak of (401) was used is that the reflection has no preferred orientation and the position of the 2θ does not overlap with those of C-S-H,

tobermorite, hillebrandite and α -quartz. The intensities of the (401) reflections of each experiment are shown in Table 4.

First, the effect of the crystalline state of the starting materials of silica on the formation rate of xonotlite will be examined. In the runs at 191°C using Brazilian quartz, xonotlite begins to appear in four hours and at the same time tobermorite gradually transforms into xonotlite. In the runs using silica gel (reagent), on the other hand, xonotlite begins to appear relatively later, i.e., after eight hours, but once xonotlite is formed, crystallization of the mineral proceeds rapidly and the degree of crystallization after 168 hours in the latter runs is higher than that of the former reaction.

Secondly, the reaction temperature which affects seriously the formation rate of xonotlite was examined. At 214°C in four hours, xonotlite begins to appear while eight and twenty four hours are required at 191°C and 175°C, respectively. Such temperature dependence has

TABLE 4. CRYSTALLIZATION RATE OF XONOTLITE.

Form of SiO ₂	Form of Al ₂ O ₃	Reaction condition			Diffraction intensity of X(401) (%)
		Temp.(°C)	Press.(kg/cm ²)	Time (h)	
Brazilian quartz	—	191	12	2	0
				4	13.2
				6	30.5
				8	35.6
				24	77.0
				168	81.6
Silica gel (reagent)	—	175	8	12	0
				24	62.1
				48	81.6
				2	0
				4	0
				6	0
		191	12	8	43.1
				24	78.2
				168	100
		214	20	1	0
				2	0
				4	80.5
Silica gel (reagent)	γ -Al ₂ O ₃	191	12	8	0
				12	0
				24	72.4
				168	79.3
	Kaolin	191	12	8	0
				12	49.4
				24	57.5
				168	73.6

been already confirmed by Kubo et al. (1974b) in their experiments used industrial raw materials.

Effects of the addition of Al₂O₃ were finally examined. At 191°C, xonotlite is formed in eight hours in the runs without adding Al₂O₃, while the formation of xonotlite is retarded by adding a small quantity of Al₂O₃, e.g., twenty-four hours with addition of γ -Al₂O₃ (reagent), and twelve hours with Kaolin clay, respectively as are seen in Table 4.

It may be concluded that formation of xonotlite begins earlier in the runs when Brazilian quartz is used than that of silica gel (reagent). However, rate of crystallization is faster in the case of silica gel. Further, the formation rate of xonotlite is exponentially increased as the reaction temperature is raised. The addition of Al₂O₃ retards the crystallization of xonotlite about 1–3 times.

C. LATTICE CONSTANTS

As mentioned above formation processes of minerals including C-S-H are different from each other in the three systems of different starting materials. In order to examine the effects of experimental conditions on the crystal structure of xonotlite, the most predominant phase, lattice constants of the mineral were investigated. X-ray diffraction measurements were performed under the same conditions as mentioned before. Silicon powder of NBS was used as the internal standard. Typical examples of the powder data are shown in Table 5 and the calculation of lattice constants was done using the compu-

ter program of RSLC-3 (Sakurai, 1967) and the results obtained are summarized in Table 6.

Although the process of growth of xonotlite varies with the crystalline state of the starting material of silica such as, Brazilian quartz or silica gel, as mentioned above, the lattice constants of xonotlite are almost constant regardless of the crystalline state of the starting material within the measurement error. These results agree well with those of synthetic xonotlite formed at 400°C for two days at the atomic ratio of Ca/Si of 1.00 in α -quartz(SiO₂)-CaO-H₂O system (Kalousek et al., 1977) and of natural xonotlite (Taylor, 1954 and Imai et al., 1972).

Furthermore, the lattice constants are independent of addition of Al₂O₃ and the chemical form of aluminum such as γ -Al₂O₃ and clay containing mainly kaolin mineral.

As a result, it was found that the lattice constants of xonotlite keep almost constant regardless of crystalline state of starting material, addition of aluminum, and formation temperature.

D. SELECTED AREA ELECTRON DIFFRACTION AND TRANSMISSION ELECTRON MICROSCOPIC OBSERVATIONS

As mentioned before, amorphous to semi-crystalline C-S-H is always produced at the initial stage of reaction and is transformed to fine crystals of several phases.

Since the products are mixture of different state of crystalline phases, it is extremely difficult to identify the constituent phases only by X-ray powder diffraction method. Therefore, the products were examined in further detail by selected area electron diffraction method and scrutinized as to how they were transformed into xonotlite. The sample was dispersed under the ultrasonic wave because the products are generally fine agglomerates and/or the spherical secondary particles.

The typical examples of selected area electron diffraction patterns and electron microphotographs are shown as a function of starting materials in the order of reaction process in Plates 1, 2 and 3. In the following, details of the observed phases will be described.

1. C-S-H

C-S-H is always produced at the initial stage of all experimental conditions as was confirmed by X-ray diffraction method. Two types of C-S-H are distinguished in the electron diffraction patterns. The one is C-S-H showing broad diffraction rings whose d-spacings correspond to those of (220) and (040) of tobermorite, respectively. The diffraction ring corresponding to (040) is usually dim. The other is C-S-H showing spread diffraction spots corresponding to (220) and (040) of tobermorite. The former type is formed in silica gel (reagent SiO₂)-CaO-H₂O and silica gel (reagent SiO₂)-CaO-Al₂O₃-H₂O systems as shown in Plate 2b.

This type characteristically exhibits crumpled foil shown in Plate 2a and/or fibre shown in Plate 2c. The latter type is observed in all systems as is shown in Plate 3b with the form of fibre shown typically in Plates 1a and 3a. The fibre in the Brazilian quartz system is as short as 2 μ m or less as shown in Plate 1a, while that in the system of silica gel (reagent SiO₂) is relatively long. Fibres

TABLE 5. X-RAY POWDER DIFFRACTION DATA FOR XONOTLITE.

Sample	(1)			(2)			(3)			(4)		
hk ℓ	d (obs.)	d (calc.)	I/I ₁ (obs.)	d (obs.)	d (calc.)	I/I ₁ (obs.)	d (obs.)	d (calc.)	I/I ₁ (obs.)	d (obs.)	d (calc.)	I/I ₁ (obs.)
200	8.55	8.54	4	8.55	8.53	5	8.55	8.53	5	8.55	8.53	6
001	7.03	7.01	16	7.04	7.01	23	7.03	7.01	16	7.03	7.01	18
400	4.260	4.268	29	4.264	4.265	27	4.266	4.267	28	4.262	4.266	30
401	3.639	3.633	31	3.644	3.636	40	3.644	3.634	38	3.642	3.634	41
002	3.508	3.504	4	3.516	3.506	6	3.508	3.504	3	3.505	3.503	4
202	3.235	3.233	33	3.249	3.237	47	3.231	3.234	36	3.230	3.234	40
320	3.088	3.088	100	3.087	3.089	100	3.089	3.088	100	3.087	3.088	100
321	2.829	2.821	40	2.830	2.824	48	2.830	2.822	42	2.829	2.822	46
402	2.704	2.698	25	2.710	2.702	36	2.708	2.700	28	2.710	2.700	35
601	2.634	2.629	5	2.637	2.630	6	2.634	2.630	5	2.635	2.630	6
122	2.506	2.507	18	2.510	2.509	20	2.508	2.507	20	2.507	2.507	20
003	2.342	2.336	7	2.344	2.337	16	2.341	2.336	9	2.342	2.336	10
203	2.253	2.249	6	2.258	2.252	9	2.255	2.249	8	2.254	2.249	9
801,522	2.036	2.037, 2.031	19	2.038	2.037, 2.033	24	2.036	2.037, 2.031	22	2.036	2.037, 2.032	25
721	1.9509	1.9485	27	1.9517	1.9495	32	1.9513	1.9488	36	1.9521	1.9487	35
040	1.8389	1.8378	20	1.8385	1.8399	23	1.8406	1.8381	20	1.8403	1.8382	22
041	1.7783	1.7777	3	1.7776	1.7797	3	1.7802	1.7780	3	1.7802	1.7780	3
722	1.7557	1.7532	6	1.7566	1.7549	7	1.7573	1.7536	8	1.7570	1.7538	8
204	1.7101	1.7138	10	1.7115	1.7155	13	1.7092	1.7139	12	1.7089	1.7139	14
920,133	1.6842	1.6857, 1.6818	5	1.6833	1.6851, 1.6834	6	1.6853	1.6855, 1.6818	6	1.6848	1.6850, 1.6819	7
1001	1.6554	1.6558	3	1.6548	1.6557	4	1.6559	1.6559	5	—	1.6556	—
242	1.5997	1.5978	4	1.5999	1.5996	5	1.6004	1.5980	4	1.6002	1.5981	4
124,541	1.5747	1.5739, 1.5756	3	1.5769	1.5753, 1.5771	5	1.5745	1.5739, 1.5758	4	1.5745	1.5738, 1.5759	4
324,514	1.5214	1.5212, 1.5205	7	1.5223	1.5230, 1.5225	8	1.5220	1.5214, 1.5208	8	1.5220	1.5215, 1.5211	9
1201,450	1.3923	1.3922, 1.3901	5	1.3916	1.3920, 1.3914	5	1.3919	1.3922, 1.3902	6	1.3916	1.3919, 1.3903	6
543	1.3261	1.3281	3	1.3285	1.3298	4	1.3269	1.3283	4	1.3273	1.3285	5
650	1.3059	1.3062	3	1.3087	1.3071	4	1.3059	1.3063	3	1.3059	1.3063	4
244	1.2527	1.2534	2	1.2545	1.2547	3	1.2537	1.2535	3	1.2540	1.2536	3
652	1.2213	1.2225	2	1.2235	1.2239	3	1.2215	1.2228	3	1.2217	1.2229	3

- (1) Brazilian quartz-CaO-H₂O system.
- (2) Silica gel (reagent)-CaO-H₂O system.
- (3) Silica gel (reagent)-CaO- γ -Al₂O₃-H₂O system.
- (4) Silica gel (reagent)-CaO-Kaolin-H₂O system.

obtained at 191°C or lower temperatures in the system of silica gel (reagent SiO₂)-CaO-H₂O are characterized by aggregating in bundles (Plate 2c).

2. TOBERMORITE

Tobermorite is recognizable only in Brazilian quartz-CaO-H₂O system and silica gel (reagent SiO₂)-CaO-Al₂O₃-H₂O system. Extremely dim diffraction spots are observed at $k = \text{odd}$ which have not been recognized by X-ray powder diffraction method and the diffraction spots at $h + k = 2n$ are commonly observable as

shown in Plates 1c and 3d. Two morphological types of tobermorite are distinguishable under the electron microscope. The one is the form of irregular plate whose end is partly splitted as shown in Plate 1b. This type is observed in the Brazilian quartz system. The other is euhedral platy crystals found in the reaction added Al₂O₃ (Plate 3c).

3. HILLEBRANDITE

Hillebrandite is recognized only in the reaction at 191°C or higher temperatures in silica gel (reagent SiO₂)-

TABLE 6. LATTICE PARAMETERS OF XONOTLITE.

Sample	Ca/Si	Al/Si	Reaction condition		a d(Å)	b d(Å)	c d(Å)	β (°)
			Temp(°C)	Time(day)				
(1)	1.00	—	191	7	17.07	7.35	7.01	90.4
(2)	1.00	—	191	7	17.06	7.36	7.01	90.3
(3)	1.00	0.025	191	7	17.07	7.35	7.01	90.4
(4)	1.00	0.025	191	7	17.06	7.35	7.01	90.3
(5)	1.00	—	400	2	17.03	7.36*	7.01	90.3
(6)	—	—	—	—	17.05	7.36	7.01	≈ 90
(7)	—	—	—	—	17.00*	7.32	7.05	90 \pm 1
(8)	1.12	0.12	300	7	17.07	7.38*	6.98	89.7

* The dimension of unit cell is arranged for reference.

(1) Brazilian quartz-CaO- H_2O system.

(2) Silica gel (reagent)-CaO- H_2O system.

(3) Silica gel (reagent)-CaO- γ - Al_2O_3 - H_2O system.

(4) Silica gel (reagent)-CaO-Kaolin- H_2O system.

(5) Synthetic xonotlite (Kalousek et al., 1977).

(6) Xonotlite from Hashidate, Japan (Umai et al., 1972).

(7) Xonotlite from Tetela de Xonalta, Mexico (Taylor, 1954).

(8) Synthetic xonotlite (Kalousek et al., 1977).

CaO- H_2O system as has been identified by X-ray powder diffraction method. Since the mineral shows strong preferred orientation parallel to (001), only electron diffraction patterns concerned to a^* and b^* were obtained. In the diffraction patterns, $k = \text{odd}$ layer is usually absent and/or accompanied with extremely dim streaks, and diffraction spots of higher order are completely absent as shown in Plate 2f. Therefore, hillebrandite is regarded as the state of lower degree of crystallization. The characteristic prism form of hillebrandite is shown in Plate 2e.

4. XONOTLITE

Xonotlite is the final product as the equilibrium phase in all systems as was confirmed by X-ray powder diffraction method. An extremely sharp streak parallel to a^* in the layer of $k = \text{odd}$ is observed in the electron diffraction pattern and the diffraction spots at $2h + k = 4n$ are usually observable as shown in Plates 1f and 3f. Two types of xonotlite, strip-shaped and needle-shaped, are distinguishable by electron microscopic observations. The strip-shaped xonotlite is mainly found at the initial stage of Brazilian quartz (SiO_2)-CaO- H_2O system as shown in Plate 1d and then it transforms to the needle-shaped one with the duration of time (Plate 1e). The needle-shaped xonotlite is also found in the silica gel (reagent) system (Plate 3e). It is to be noted that in the silica gel (reagent SiO_2)-CaO- H_2O system at 191°C or lower temperatures, most of the needle-shaped xonotlite form bundled aggregates and some of them reach as large as approximately 2 μm in width as shown in Plate 2d.

E. SPECIFIC SURFACE AREA AND IGNITION LOSS

It is well known that the state of crystal growth, especially the size of crystal, can be expressed as the specific surface area (Kalousek, 1955; Takahashi et al., 1972b and 1973 and Hara et al., 1979). The degree of crystal growth of the experimental products was examined by this method. The specimens were dried at 90°C for twenty four hours and then the specific surface area was measured by BET method using a P-700 type manufactured by Shibata Chemical Instrument Co. The results obtained are shown in Table 7.

TABLE 7. SPECIFIC SURFACE AREA OF THE EXPERIMENTAL PRODUCTS.

Starting material of SiO_2	Starting material of Al_2O_3	Reaction condition			Specific surface area (m^2/g)
		Temp.(°C)	Press.(kg/cm ²)	Time(h)	
Brazilian quartz	—	191	12	2	130
				4	119
				6	67
				8	61
				24	53
Silica gel (reagent)	—	191	12	2	109
				4	113
				6	84
				8	69
				24	50
Silica gel (reagent)	γ - Al_2O_3	191	12	1	107
				2	97
				4	38
				8	110
				12	109
Silica gel (reagent)	Kaolin	191	12	24	57
				8	100
				12	54
				24	49

Values of the specific surface area are, in general, about 100 m^2/g or more at the initial stage of reaction. With increasing crystallization of xonotlite, the value decreases gradually and finally goes down to 40 to 60 m^2/g .

Ignition loss of xonotlite obtained after 7-days reaction at 191°C in Brazilian quartz (SiO_2)-CaO- H_2O and silica gel (reagent SiO_2)-CaO- H_2O systems was also examined. After heating at 1000°C for three hours, ignition loss of xonotlite of the former system was 4.1% and that of the latter system was 3.8%, both values almost coincide with each other. These values are larger than that calculated from the ideal chemical formula, $\text{Ca}_6(\text{Si}_6\text{O}_{17})(\text{OH})_2$, of xonotlite, 2.46%. The fact agrees well with the result obtained by Kalousek et al. (1977). They suggested that xonotlite contains more water than that contained in the ideal formula. After heating over 1000°C, complete transformation of xonotlite to β -wollastonite was confirmed in all experiments.

IV. MORPHOLOGY AND TEXTURE, AND ITS RELATIONSHIPS TO THE INDUSTRIAL PRODUCTS

Morphological and textural relationships of the experimental products were examined by means of stereoscope and scanning and transmission electron microscopes.

For the stereoscopic observations, the specimens were dried, and the characteristics of the surface were examined. Further detailed observations were performed by scanning and transmission electron microscopes. Some typical examples are shown in Plates 4, 5 and 6 in the order of reaction processes. For comparative studies, products from the industrial raw materials were also examined. The specimens were fixed with n-butyl methacrylate resin and thin plates of approximately 3 μm thick were cut off by a microtome and the inside of the plate was observed by the stereoscope. Some typical examples are shown in Plate 7. Results obtained will be summarized in the following:

1. MASSIVE AGGLOMERATE I

Massive agglomerate I is defined under the stereoscope as a dense aggregate of fine, angular particles of 20 to 130 μm in diameter. Observations by scanning electron microscope reveal that the aggregate is composed of fibre crystals of several microns as shown in Plate 4a. Massive agglomerate I is formed at the initial stage of reaction of Brazilian quartz (SiO_2)-CaO- H_2O system and gradually becomes round with duration of time. Most of surface angles of the agglomerate are rounded off in four hours. Besides the fibre crystals, plate crystals of several microns are also formed. Fibre crystal and plate crystal were identified as C-S-H and tobermorite, respectively.

2. MASSIVE AGGLOMERATE II

The particle size of massive agglomerate II is 5 to 50 μm , slightly smaller than that of massive agglomerate I. The shape is irregular and the coarse aggregate is composed of fine crystals as shown in Plates 5a and 6a. Massive agglomerate II is formed at the initial stage of reaction of silica gel (reagent) system. Electron microphotographs show that coarse and granular aggregate composed of fine crumpled foil crystals of several microns is covered by fibre crystals of several to 20 μm and/or these bundled aggregates as is shown in Plates 5b and 6b. In some cases, tangles of prism crystals of several to 20 μm are observed between and around the particulate aggregates as shown in Plate 5e.

The former is formed in the experiments at 191°C or lower temperatures in the reactions of silica gel (reagent SiO_2)-CaO- H_2O and silica gel(reagent SiO_2)-CaO- Al_2O_3 - H_2O systems. Only few bundled aggregates of fibre crystals are found in the reaction with Al_2O_3 addition. The tangles of prism crystals are mainly found at higher temperature in the silica gel (reagent)-CaO- H_2O system.

It should be mentioned in relation to the spherical secondary particles that the massive agglomerate containing few bundled aggregates, axiolitic or prism crystals become gradually spheritic with the lapse of time, while bundled aggregates show no morphological change.

The crumpled foil and fibre crystal are identified as C-S-H and the prism is hillebrandite, respectively.

3. NEEDLE AGGLOMERATE

Needle agglomerate is defined as the agglomerate composed of mainly needle crystals of 5 to 20 μm accompanying a few irregular-shaped aggregates as shown in Plate 5c. By the examination of scanning electron microphotographs, it is determined that the needle agglomerate consists of the bundled aggregates of fine needle crystals of about 20 μm long with 1 μm wide or less. In some cases, irregular-shaped aggregates of needle crystals are found as are shown in Plate 5d. The needle agglomerate is characteristically found in the runs at 191°C or lower temperatures in the silica gel (reagent SiO_2)-CaO- H_2O system when massive agglomerate II does not gather forming spherical secondary particles with duration of time.

The needle crystal is confirmed as xonotlite.

4. SPHERICAL SECONDARY PARTICLE A

Surface observations of the experimental products

under the stereoscope indicate that two types of the spherical secondary particles are generally formed, i.e., particle A is 20 to 130 μm and particle B, 10-50 μm . Type A can be further classified into oolitic particle including an irregular-shaped mass (A_1), spherical-shelled particle (A_2) and dense aggregate of fine particles (A_3). The spherical secondary particle A_1 and A_2 are formed from the massive agglomerate I in the reaction of Brazilian quartz system with the lapse of time. In runs after six hours, A_1 and A_2 coexist together as shown in Plate 4b. A_1 is transformed into A_2 as the reaction proceeds and completely transformed into A_2 in eight hours as shown in Plate 4c. A part of A_2 is broken after twenty four hours.

Detailed observations by scanning and transmission electron microscopes show that the inside of oolitic particle (A_1) is partly hollowed and strip or needle crystals of several microns long with 1 μm wide or less are densely aggregated on the inner rough surface as shown in Plate 4c. Moreover, needle crystals of 1 μm long or less project on the surface of the particles like a brush as shown in Plate 4d.

The spherical shell shaped particle (A_2) is completely hollow and the uniform shell with several microns thickness is commonly developed. The shell is composed of dense aggregates of fine needle crystals of several microns long and 1 μm wide or less as shown in Plate 4f. The length of needle crystals projecting on the surface of particle is as short as 1 μm or less.

Oolitic and spherical shell shaped secondary particles are also found in the industrial silica powder (α -quartz) system as shown in Plate 7a. Transformation of these particles into dense aggregates of fine particles (A_3) is accelerated, as the grain-size of CaO crystals of the starting materials (Plate 7c) is increased, and simultaneously, the size of the secondary particle is increased. Observation of the cross-section of the spherical-shelled particle by stereoscope indicates that the particle is completely hollow similarly to that produced in the Brazilian quartz system and the thickness of the particle shell is about 2 to 6 μm as shown in Plate 7b. Dense aggregates of fine crystals (A_3) are, on the other hand, found in the runs when sintered CaO crystals are used. The whole secondary particle is uniformly packed with fine crystals as shown in Plate 7d. Scanning and transmission electron microphotographs indicate that the particle is composed of dense aggregates of fine needle crystals and the length of needle crystals projecting on the surface of particle is as short as 1 μm or less as shown in Plates 4g and 4h.

The fine strip and needle crystals are confirmed as xonotlite.

5. SPHERICAL SECONDARY PARTICLE B

Spherical secondary particle B is almost spherical but some what angular particles of 10 to 50 μm in size, and is a little smaller than the spherical secondary particle A. The particle is composed of coarse aggregates of fine crystals as shown in Plates 5f and 6c. Scanning and transmission electron microscopic observations show that spherical secondary particle B consists of two types of aggregates. The one is extremely coarse aggregates of needle crystals of 2 to 4 μm long projected on the surface (B_1) as shown in Plates 5g and 5h. The other (B_2) is, as

shown in Plate 6d, some coarse aggregates of needle crystals. The particle is unevenly hollow and the inner surface of the sphere is covered partially with long bundled aggregates of needle crystals as shown in Plate 6e. The needle crystals as short as 1 to 2 μm long project on the outer surface as shown in Plate 6f. B₁ corresponds to the particle which is spherized with the lapse of time among the massive agglomerate II and is formed at 214°C in the silica gel (reagent SiO₂)-CaO-H₂O system. B₂ is found in the silica gel (reagent SiO₂)-CaO-Al₂O₃-H₂O system and is similar to the products in the industrial by-product silica (amorphous) system. The inner surface of particle is rough and the thickness of particle shell is about 2 to 12 μm as shown in Plates 7e and 7f. All of these needle crystals forming particle B are xonotlite.

6. MORPHOLOGICAL RELATIONSHIPS TO THE INDUSTRIAL PRODUCTS

Morphology and texture of the spherical secondary particles have intimate relations to the physical properties of the industrial materials.

As mentioned above, the process of crystal growth is varied with crystalline state of the starting material and reaction temperature. Most of the products transform into spherical secondary particles through complicated forms of aggregates. The forms of aggregates are summarized in Table 8. The industrial products together with forms of spherical secondary particle were already investigated in detail by the present author and the results were summarized in the previous papers (Shibahara et al., 1986a and b). The industrial spherical secondary particle is also composed of xonotlite and is roughly classified into two types. The one is the spherical secondary particle defined as A in the present experiment, i.e., oolitic particle (A₁), spherical-shelled particle (A₂) and dense aggregate of needle crystals of xonotlite (A₃). The other defined as B is a little smaller than A and is characterized by the long needle crystals of xonotlite projecting on the surface of the particle. B can be further divided into B₁ and B₂, i.e., extremely coarse

aggregate of needle crystals (B₁) and somewhat coarse, hollow aggregate (B₂). Spherical secondary particles A₁, A₂ and B are favorable to the industrial light-weighted products such as insulation and heat insulating materials. The products made of the hollow, spherical secondary particle B₂ have an advantage in high strength due to long needle crystals projecting on the surface of particle. The B₁ type has, however, a drawback that the contraction occurs largely during the process of drying. This is caused by extremely coarse aggregate of the long needle crystals which project on the surface of particle.

Among A, the particle (A₃) in which xonotlite is densely aggregated is suited for high-density products including fire-resistant building material. Even though the needle crystals of xonotlite are produced, however, it should be noted that particles in which the needle agglomerate remains have drawbacks of poor mouldability and contractible and distortion properties of product during the drying process. Such particles therefore, can not be practically used.

V. FORMATION MECHANISM OF THE SPHERICAL SECONDARY PARTICLE

Formation process and mineralogical variation of the experimental products will be considered in this chapter in relation to the formation of secondary particles. Special attention was paid on the crystalline state of starting materials and experimental conditions.

(1) Brazilian quartz(SiO₂)-CaO-H₂O system: Fine fibrous C-S-H gathers around α -quartz particles to form a massive agglomerate at the initial stage of reaction as shown in Plate 4a. As the reaction proceeds, platy, irregular tobermorite begins to crystallize, and simultaneously the massive agglomerate is gradually rounded by agitation in the vessel. As the result of further crystallization, tobermorite is splitted along b-axis and xonotlite strip is formed. The morphology of xonotlite changes to needle shape. At the same time, the unreacted α -quartz in the massive agglomerate gradually dissolves and the inside of the agglomerate begins to hollow, resulting oolitic secondary particle as is shown in Plate 4c which changes to a completely hollow spherical shell shaped secondary particle (Plates 4f).

(2) Silica gel (reagent SiO₂)-CaO-H₂O system: A coarse aggregate of fine crystals consisting of crumpled foil of C-S-H is formed at the initial stage. Fibrous C-S-H (almost bundled aggregates) is usually accompanied with the aggregate forming irregular massive agglomerate as is shown in Plate 5b. C-S-H composed of bundles of fibrous aggregate, on the other hand, remains unchanged until the transformation to needle crystal of xonotlite, which forms a bundled aggregate, so it is not rounded as shown in Plate 5d even under the agitation condition. With raising temperature, prisms of hillebrandite are partly formed in and around the massive agglomerate composed of C-S-H (Plate 5) and simultaneously bundled aggregates of fibrous C-S-H begin to disappear. Since hillebrandite disappears as formation of xonotlite, spherical secondary particles composed of extremely coarse aggregate of needle crystals of xonotlite are formed as shown in Plate 5g.

TABLE 8. MORPHOLOGICAL VARIATION OF AGGREGATES OBSERVED IN THE EXPERIMENTAL PRODUCTS.

Starting material of SiO ₂	Starting material of Al ₂ O ₃	Reaction condition			Form of aggregate
		Temp.(°C)	Press. (kg/cm ²)	Time (h)	
Brazilian quartz	—	191	12	2	Massive agglomerate I
				4	Massive agglomerate I (slightly rounded)
				6	Spherical secondary particle A (oolitic and spherical-shelled)
				8	Spherical secondary particle A (spherical-shelled)
Silica gel (reagent)	—	175	8	12	Massive agglomerate II (composed of many bundled aggregates of fibre crystals)
				24,48	Needle agglomerate
	—	191	12	2,4,6	Massive agglomerate II (composed of many bundled aggregates of fibre crystals)
				8,24	Needle agglomerate
	—	214	20	1,2	Massive agglomerate II (tangle of prisms)
				4	Spherical secondary particle B (coarse aggregate of needle crystals)
Silica gel (reagent)	γ -Al ₂ O ₃	191	12	8,12	Massive agglomerate II (composed of less bundled aggregates)
				24	Spherical secondary particle B (hollow)
	Kaolin	191	12	8	Massive agglomerate II (composed of less bundled aggregates)
				12,24	Spherical secondary particle B (hollow)

As mentioned above, distinct differences are recognized in the crystal growth and aggregating processes between the two systems depending upon the crystalline phase. In other words, the difference largely depends upon the morphology of aggregate of C-S-H formed at the initial stage of the reaction. This can probably be explained by the fact that the solubilities of α -quartz and silica gel in water are different from each other, namely, that of silica gel at 191°C is four times more than that of α -quartz (Kennedy, 1950). In the silica gel system, therefore, nucleation occurs possibly at numerous sites at the initial stage of the reaction, so many irregular massive agglomerates may be formed. In the Brazilian quartz system, on the other hand, nucleation site is relatively limited so that C-S-H densely gathers around the particle of α -quartz to form a dense massive agglomerate. As the reaction proceeds, the C-S-H is transformed to tobermorite and to almost pure xonotlite in the α -quartz and silica gel systems, respectively. This fact can also be interpretable based on the solubility difference. In the highly soluble silica gel system, effective ratio of Ca/Si in the solution is nearly equal to that in the starting material (the ratio is equivalent to that of xonotlite), i.e., 1.00, while the ratio must be far less than 1.00 in the α -quartz system. Since the ratio of Ca/Si in tobermorite is in the range between 0.75 and 1.00 (Hamid, 1979), the crystalline phase formed at the initial stage should be tobermorite in the α -quartz system.

(3) In the silica gel (reagent SiO_2)-CaO- Al_2O_3 - H_2O system, either the form of aluminum is γ - Al_2O_3 or kaolin (clay), coarse aggregates of fine, crumpled foil of C-S-H forming particles entangled with fibrous C-S-H are generally formed at the initial stage of reaction resulting irregular massive agglomerates as are shown in Plate 6b. With proceeding reaction, platy tobermorite begins to crystallize which later transforms to needle xonotlite, and simultaneously unevenly hollow spherical secondary particles composed of xonotlite are formed as are shown in Plates 6d and 6e.

By addition of Al_2O_3 to the system, length of each C-S-H fibre is shortened and the number of bundled aggregates are extremely reduced. Al is probably substituted for Si in the Si-O dreier ketten in the crystal structure of C-S-H as was indicated by Toraya et al. (1985) and as a result, the dreier ketten is cut resulting short fibres and decreasing number of the bundled aggregates. Concerning tobermorite, Kalousek (1957), Diamond et al. (1966) and Petrovic (1969) suggested the existence of Al-Si substituted tobermorite. With further reaction, the needle crystal of xonotlite is slightly shortened and the number of the bundled aggregates are sharply decreased. This may be caused by the addition of Al_2O_3 , but change of lattice constants caused by the substitution is not confirmed in the present experiments.

In the experiments using the industrial by-product silica (amorphous), the spherical secondary particles with the same texture and morphology as those formed in the silica gel (reagent) system with Al_2O_3 addition were also confirmed. This is probably caused by Al_2O_3 content more or less in the industrial raw materials.

Comparing the results reported by Kubo et al. (1974b), who used industrial silica powder (α -quartz) containing Al_2O_3 as impurity, with the present experimental results obtained by using Brazilian quartz, no

essential difference can be found concerning the formation process of the spherical secondary particles. This is probably caused by the fact that C-S-H gathers around the non-reacted grain of α -quartz even under the condition of Al existence resulting low silica solubility at the initial stage of reaction (Sakiyama et al., 1977). Thus, the morphology of massive agglomerate of C-S-H is almost similar in the two cases in relation to the spherical secondary particles.

As a result, the presence of Al_2O_3 is of use for producing the industrially useful spherical secondary particles composed of xonotlite, though it retards the reaction speed as was indicated by Takahashi et al. (1973) and El-Hemaly et al. (1977).

VI. SUMMARY

The active slurry method which is commonly used in the industrial field, is quite effective for the formation of the spherical secondary particles composed of xonotlite in the SiO_2 -CaO- H_2O system. In other words, the epoch-making active slurry method is characterized by the formation of the spherical secondary particles. Therefore, basic researches on the formation mechanism of the secondary particles have been desired, though Kubo et al. (1974b) have reported some preliminary experiments using industrial raw materials.

The main results obtained in the present experiments are summarized as follows:

1. The reaction products were identified precisely by X-ray powder diffraction and electron diffraction methods. Detailed textural and morphological relations of the products were examined in relation to the formation processes of aggregates as well as the secondary particles by stereoscope and scanning and transmission electron microscopes.

2. The final products are composed of xonotlite and the morphology of aggregate of the xonotlite largely depends upon the crystalline state of C-S-H, which is commonly formed at the initial stage of the reaction.

3. Growth rate of crystalline phase was examined by X-ray powder diffraction method on both Brazilian quartz and silica gel (reagent) systems. In the former system, C-S-H is formed at first and transforms gradually to xonotlite through the stage of tobermorite. In the latter, however, xonotlite is rapidly crystallized directly from C-S-H after certain incubation period.

4. The addition of small quantity of aluminum in the form of Al_2O_3 to the silica gel (reagent) system shortens the length of fibrous C-S-H and the number of bundled aggregates is reduced. Once xonotlite is crystallized, unevenly hollow spherical secondary particles accompanied with long needle xonotlite on the surface (B_2) begin to form.

5. The texture and morphology of the spherical secondary particle formed in the system of industrial by-product silica (amorphous) system are similar to those formed in the silica gel (reagent) system with Al_2O_3 addition.

6. The lattice constants of xonotlite crystallized at various stages and systems were examined, but no significant difference was confirmed.

7. Although the addition of small amount of Al_2O_3

retards the formation stage of xonotlite, the fact shows favorable results for the formation of the spherical secondary particles, since bundled aggregates of fibrous C-S-H are formed less.

8. The oolitic (A_1) and spherical shell shaped (A_2) secondary particles composed of xonotlite are also produced in the industrial silica powder (α -quartz) system. As the particle size of the starting CaO is increased, the spherical secondary particle becomes denser and denser and the morphology changes to dense aggregate of needle crystals of xonotlite (A_3) from spherical shell shaped through oolitic.

9. The spherical secondary particle A (A_1 and A_2) and B (B_1 and B_2) are suited for the light-weighted products. Since the hollow spherical secondary particle (B_2) has long needle crystals on the surface of particle, the industrial strength of the moulded product is high. The product manufactured from the spherical secondary particles composed of extremely coarse aggregates of needle crystals (B_1) shows the large contraction after drying.

10. The spherical secondary particles composed of dense aggregates of needle crystals of xonotlite (A_3) are suited for high-density products.

11. Non spherical aggregates formed by needle xonotlite have drawback characteristics such as poor mouldability and contraction and distortion during the drying process.

The knowledge obtained in the present research on the texture and morphology of the spherical secondary particle will surely help to improve the quality of the industrial product. That is, the most favorable conditions for producing industrial products with high quality, such as starting materials and temperatures and pressures can be determined based on the present results.

References

- AITKEN, A. and TAYLOR, H. F. W. (1960): Hydrothermal reactions in lime-quartz pastes. *J. Appl. Chem.* 10, 7-15.
- AKAIWA, S., HARADA, S. and SUDOH, G. (1956): Hydrothermal reaction products of the system CaO - SiO_2 - H_2O (in Japanese). *Semento Gijutsu Nenpo* 10, 14-23.
- ASSARSSON, G. O. (1957): Hydrothermal reactions between calcium hydroxide and amorphous silica; the reactions between 180 and 220°. *J. Phys. Chem.* 61, 473-479.
- (1958): Hydrothermal reactions between calcium hydroxide and amorphous silica; the reactions between 120 and 160°. *ibid.* 62, 223-228.
- BERMAN, H. (1937): Constitution and classification of the natural silicates. *Am. Mineral.* 22, 342-408.
- CHAN, C. F., SAKIYAMA, M. and MITSUDA, T. (1978): Kinetics of the CaO -quartz- H_2O reaction at 120° to 180°C in suspensions. *Cem. Concr. Res.* 8, 1-6.
- CIACH, T., DYCZEK, J., PETRI, M. and WESTFAL, L. (1980): Materials from the synthetic tobermorite. 7th Int. Congr. Chem. Cem. vol. 2. II. 188-191.
- DIAMOND, S., WHITE, J. L. and DOLCH, W. L. (1966): Effects of isomorphous substitution in hydrothermally-synthesized tobermorite. *Am. Mineral.* 51, 388-401.
- EAKLE, A. S. (1921): Jurupaite—A new mineral. *Am. Mineral.* 6, 107-109.
- EL-HEMALY, S. A. S., MITSUDA, T. and TAYLOR, H. F. W. (1977): Synthesis of normal and anomalous tobermorite. *Cem. Concr. Res.* 7, 429-438.
- FLINT, E. P., McMURDIE, H. F. and WELLS, L. S. (1938): Formation of hydrated calcium silicates at elevated temperatures and pressures. *J. Res. Natl. Bur. Stand.* 21, 617-638.
- HAMID, S. A. (1979): Electron microscopic characterization of the hydrothermal growth of synthetic 11 tobermorite ($\text{Ca}_6\text{Si}_6\text{O}_{18}\cdot 4\text{H}_2\text{O}$) crystals. *J. Cryst. Growth.* 46, (3), 421-426.
- HARA, N., INOUE, N. and MATSUDA, O. (1979): Studies on the crystallization process of 11 tobermorite by X-ray line-profile analysis (in Japanese). *J. Ceramic Soc. Japan.* 87, (7), 334-340.
- HELLER, L. and TAYLOR, H. F. W. (1951): Hydrated calcium silicates, ptII. Hydrothermal reactions: lime-silica ratio 1:1. *J. Chem. Soc.* 2397-2401.
- (1953): X-ray investigation of hillebrandite. *Mineral. Mag.* 30, 150-154.
- IMAI, N., OTSUKA, R., CHIHARA, K., NAKAMURA, T. and TANAKA, K. (1972): Xonotlite from Ohmi district, Niigata prefecture, Japan. *J. Japan. Assoc. Min. Petr. Econ. Geol.* 67, 63-75.
- ISHII, T., SEN, Z. and MITSUDA, T. (1978): Hydrothermal reaction of lime-quartz system by suspension method and its mechanism (in Japanese). *Semento Gijutsu Nenpo* 32, 75-78.
- KALOUSEK, G. L. (1955): Tobermorite and related phases in the system CaO - SiO_2 - H_2O . *J. Am. Concr. Inst.* 51, 989-1011.
- (1957): Crystals chemistry of hydrous calcium silicates: I, Substitution of aluminium in lattice of tobermorite. *J. Am. Ceram. Soc.* 40, (3), 74-80.
- , MITSUDA, T. and TAYLOR, H. F. W. (1977): Xonotlite: Cell parameters, thermogravimetry and analytical electron microscopy. *Cem. Concr. Res.* 7, 305-312.
- KENNEDY, G. C. (1950): A portion of the system silica-water. *Econ. Geol.* 45, 629-653.
- KUBO, K., MINOURA, T. and YAMAGUCHI, G. (1974a): Xonotlite slurry and molded material from it (in Japanese). *J. Ceramic Soc. Japan.* 82, (3), 171-175.
- , TAKEUCHI, M., ESUMI, M., YAMAGUCHI, G. and TAMURA, H. (1974b): Formation process of spherical secondary grain of xonotlite (in Japanese). *ibid.* 82, (8), 414-419.
- , MINOURA, T. and YAMAGUCHI, G. (1974c): Tobermorite slurry and molded material from it (in Japanese). *ibid.* 82, (9), 497-501.
- , ESUMI, M. and YAMAGUCHI, G. (1976): Xonotlite heat-insulating material with bulk density of 0.1 (in Japanese). *ibid.* 84, (1), 23-28.
- and TAKAGI, S. (1978): Structural form of spherical secondary particles of calcium silicate hydrate crystals and mechanical strength of the molded product (in Japanese). *ibid.* 86, (2), 45-50.
- (1980): Calcium silicate insulation (in Japanese). *Nenryo Nensho* 47, (10), 797-803.
- and SHIBAHARA, K. (1980): Synthesis of foshagite and production of molded products (in Japanese). *Gypsum & Lime.* No. 168, 249-254.
- LARSEN, E. S. (1917): Eakleite, a new mineral from California. *Am. J. Sci.* 43, 464-465.
- MAMEDOV, KH. S. and BELOV, N. V. (1955): The crystal structure of xonotlite (in Russian). *Dokl. Akad. Nauk SSSR.* 104, 615-618.
- MITSUDA, T. (1980): Hydrothermal reaction and industry of calcium silicates (in Japanese). *Ceramics in Japan.* 15, (3), 184-196.
- NAGAI, S. (1931a): Studies on hydrothermal synthesis of calcium silicates under pressure (in Japanese). *J. Soc. Chem. Ind. Japan.* 34, 619-624.
- (1931b): Studies on hydrothermal synthesis of cal-

- cium silicates under pressure (in Japanese). *ibid.* 34, 867-872.
- . (1933): Studies on hydrothermal synthesis of calcium silicates under pressure (in Japanese). *ibid.* 36, 985-991.
- OHMORI, K. (1939): Optical properties of Japanese jade (in Japanese). *J. Japan. Assoc. Min. Petr. Econ. Geol.* 22, 201-222.
- OHNO, Y. and FUJIYAMA, S. (1957): On the crystals of CaO in limestone calcined at different temperatures (in Japanese). *J. Ceramic Soc. Japan.* 65, (738), 133-136.
- PEPPLER, R. B. (1955): The system of lime, silica, and water at 180°C. *J. Res. Natl. Bur. Stand.* 54, (4), 205-211.
- PETROVIC, J., RUSNAK, V. and STEVULA, L. (1969): Isomorphous substitution of aluminium for silicon in tobermorite structure. 1. The mixtures of different froms of silicon dioxide and of different compounds of aluminium. *Chem. zvesti.* 23, 129-133.
- RAMMELSBERG, C. (1866): Uber den xonaltit, ein neues waserhaltiges kalk-silikat, und den bustamit aus Mexiko. *Z. Dtsch. Geol. Ges.* 18, 33-34.
- SAKAEDA, O. and FUJIHARA, M. (1969): Properties of quicklime obtained under different conditions of calcination (in Japanese). *Gypsum & Lime.* No. 100, 106-114.
- SAKIYAMA, M. and MITSUDA, T. (1977): Influence of aluminium on the formation of tobermorite (in Japanese). *Semento Gijutsu Nenpo* 31, 46-49.
- SAKURAI, T. (1967): Universal crystal analysis program system (in Japanese). *J. Crystallographic Soc. Japan.*
- SHANNON, E. V. (1925): An occurrence of xonotlite at Leesburg, Virginia. *Am. Mineral.* 10, 12-13.
- SHIBAHARA, K., KUBO, K. and TAKAHASHI, A. (1986a): Effects of silica raw materials on the textures of synthesized xonotlite (in Japanese). *Gypsum & Lime.* No. 202, 170-176.
- , ———, and ———. (1986b): Effects of raw lime materials on the textures of synthesized xonotlite (in Japanese). *ibid.* No. 203, 229-234.
- SPEAKMAN, K. (1968): The stability of tobermorite in the system CaO-SiO₂-H₂O at elevated temperatures and pressures. *Mineral. Mag.* 36, 1090-1102.
- TAKAHASHI, A., HAYASHI, H., MAKINO, H. and MITSUDA, T. (1972a): Morphology and thermal behaviour of poorly crystallized tobermorite (in Japanese). *Semento Gijutsu Nenpo* 26, 58-63.
- , and ———. (1972b): Effects of hydrothermal conditions on crystal growth of calcium silicate hydrate (in Japanese). *ibid.* 26, 75-84.
- , ———, and YAMAKITA, K. (1973): Effect of Al₂O₃ in hydrothermal synthesis of xonotlite (in Japanese). *ibid.* 27, 41-44.
- TAYLOR, H. F. W. (1954): The identity of jurupaite and xonotlite. *Mineral. Mag.* 30, 338-341.
- . (1964): *The Chemistry of Cements.* Academic Press. London and New York.
- TORAYA, H., KOBAYAKAWA, S. and MITSUDA, T. (1985): "Variations of texture and morphology of amorphous calcium silicate hydrate (C-S-H) according to its composition" (in Japanese). Research paper on mass transfer and variation in the bosom of the earth. 96-99.

KAZUO SHIBAHARA

OSAKA PACKING MANUFACTURING CO. LTD.,
NODASHINDEN, HOZUMI-CHO, MOTOSU-GUN, GIFU
PREF., JAPAN

EXPLANATION OF PLATE 1

Selected area electron diffraction patterns and transmission electron microphotographs of the experimental products in Brazilian quartz-CaO-H₂O system (reaction temperature: 191°C).

- Electron microscopic (EM) photograph of product after 2h.
- EM photograph (4 h).
- Selected area electron diffraction (SED) pattern of irregular platy crystal (4 h).
- EM photograph (6 h).
- EM photograph (24 h).
- SED pattern of needle crystal (24 h).

EXPLANATION OF PLATE 2

Selected area electron diffraction patterns and transmission electron microphotographs of the experimental products in silica gel (reagent)-CaO-H₂O system.

- EM photograph at 175°C, 12 h.
- SED pattern of crumpled foil at 175°C, 12 h.
- EM photograph at 175°C, 12 h.
- EM photograph at 175°C, 24 h.
- EM photograph at 214°C, 2 h.
- SED pattern of prism at 214°C, 2 h.

EXPLANATION OF PLATE 3

Selected area electron diffraction patterns and transmission electron microphotographs in silica gel (reagent)-CaO- γ -Al₂O₃-H₂O system (reaction temperature: 191°C).

- After 8 h.
- Fibre crystal after 8 h.
- After 12 h.
- Platy crystal after 12 h.
- After 24 h.
- Needle crystal after 24 h.

EXPLANATION OF PLATE 4

Stereoscopic and scanning and transmission electron microphotographs in α -quartz-CaO-H₂O system (reaction temperature: 191°C).

- | | | |
|---|---|--|
| <ol style="list-style-type: none"> Scanning electron microscopic (SEM) photograph after 2 h. Stereoscopic(S) microphotograph, 6 h. SEM photograph of the inside of the sphere, 6 h. EM photograph, 6 h. S microphotograph, 8 h. SEM photograph of the inside of the sphere, 24 h SEM photograph, 8 h. EM photograph, 8 h. | } | <p>Brazilian quartz-pure lime (calcined calcium carbonate (reagent) at 1000°C for 10 h).</p> <p>Silica powder (α-quartz)-industrial lime (calcined limestone at 1200°C for 4 h).</p> |
|---|---|--|

EXPLANATION OF PLATE 5

Stereoscopic and scanning and transmission electron microphotographs in silica gel (reagent)-CaO-H₂O system.

- 12 h at 175°C.
- 12 h at 175°C.
- 24 h at 175°C.
- 24 h at 175°C.
- 2 h at 214°C.
- 4 h at 214°C.
- 4 h at 214°C.
- 4 h at 214°C.

EXPLANATION OF PLATE 6

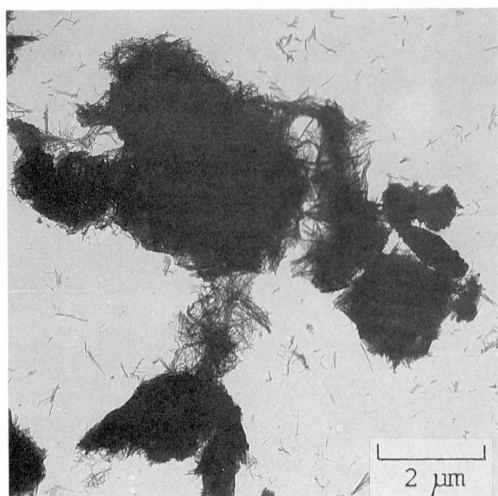
Stereoscopic and scanning and transmission electron microphotographs in silica gel (reagent)- γ -Al₂O₃-CaO-H₂O system (reaction temperature: 191°C).

- 8 h.
- 8 h.
- 24 h.
- 24 h.
- Inside of the sphere, 24 h.
- 24 h.

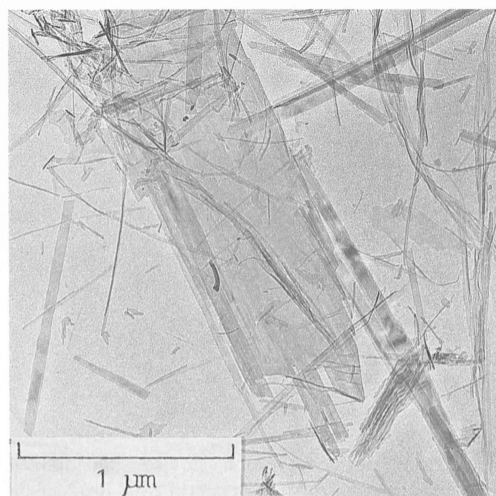
EXPLANATION OF PLATE 7

Microphotographs of spherical secondary particle formed from the industrial starting material (reaction condition: 191°C for 8 h).

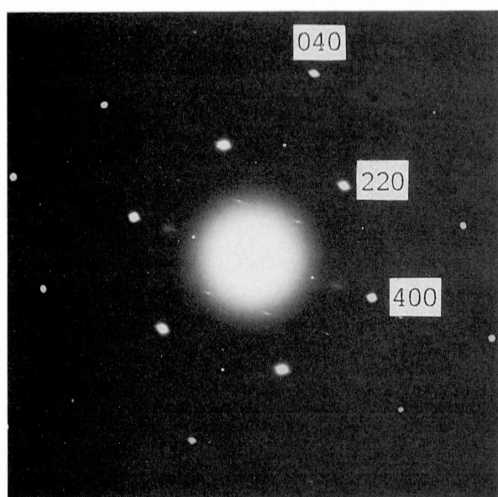
- Silica powder (α -quartz)-industrial lime (calcined at 1000°C for 4 h).
- Cross-section of a.
- Silica powder (α -quartz)-industrial lime (calcined at 1200°C for 4 h).
- Cross-section of c.
- By-product silica (amorphous)-industrial lime (calcined at 1100°C for 4 h).
- Cross-section of e.



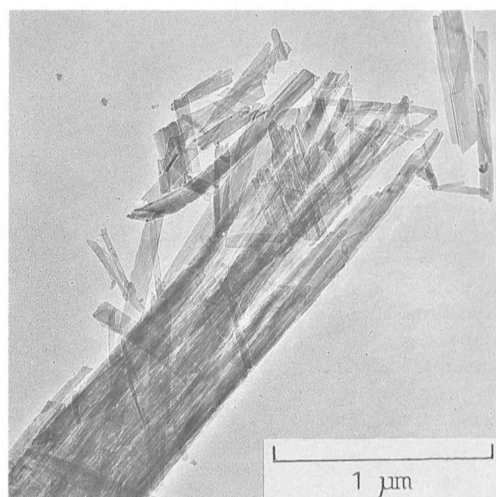
a



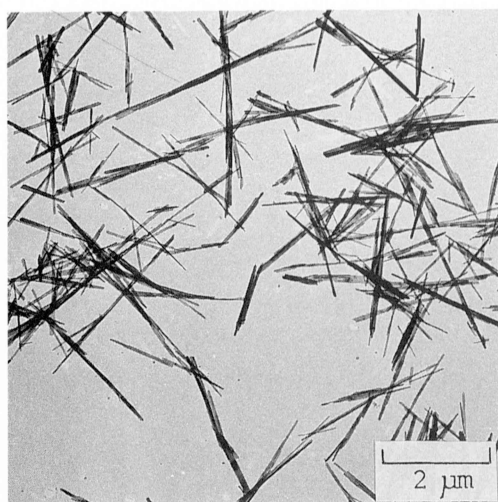
b



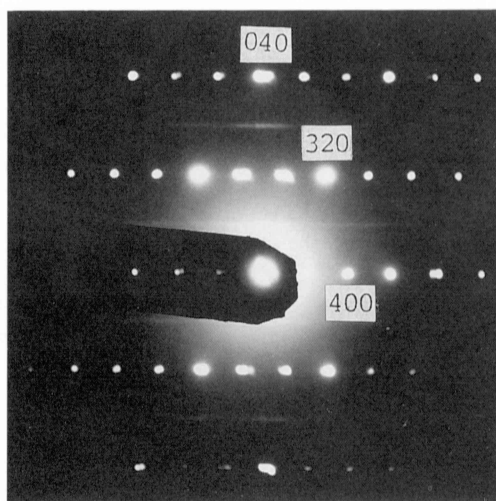
c



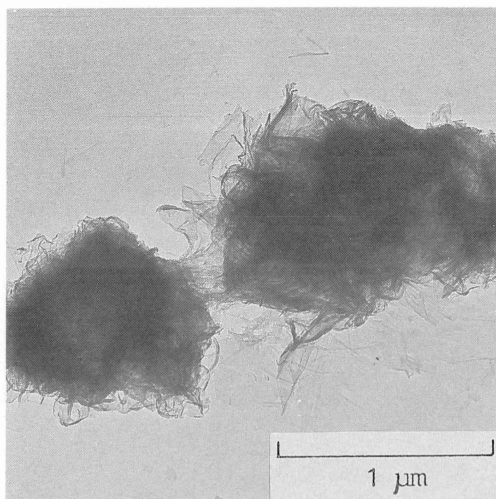
d



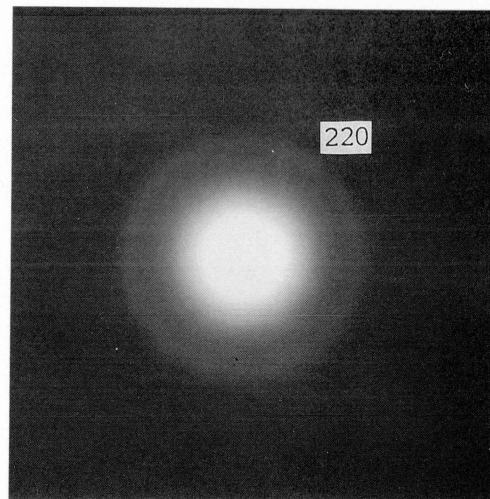
e



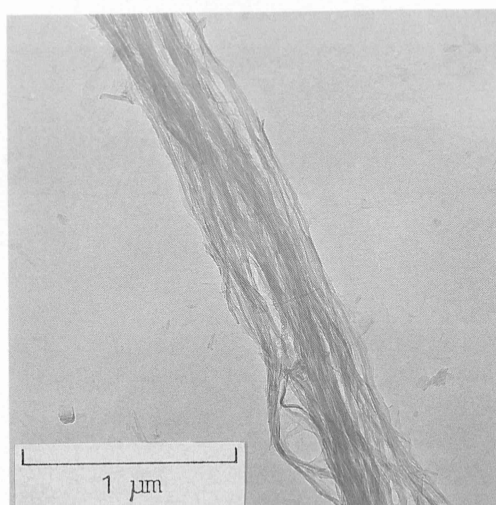
f



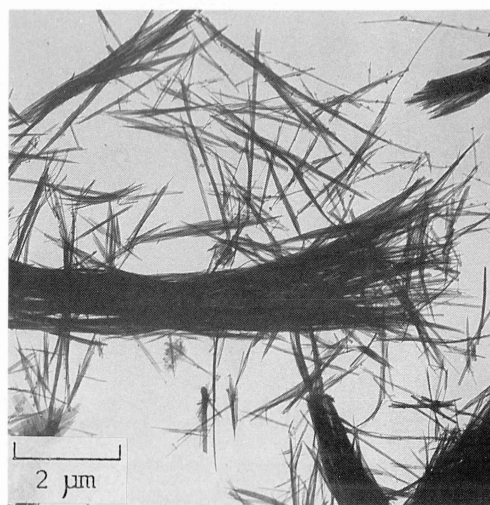
a



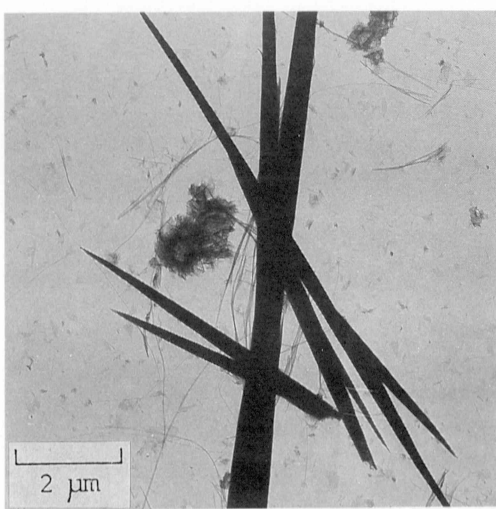
b



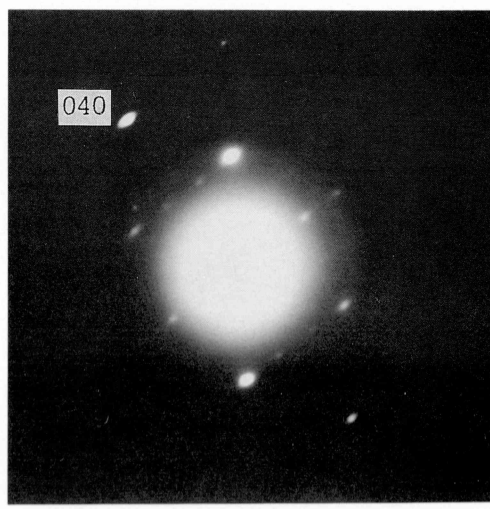
c



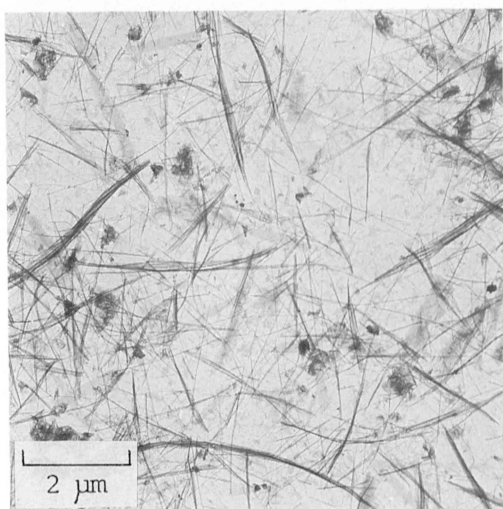
d



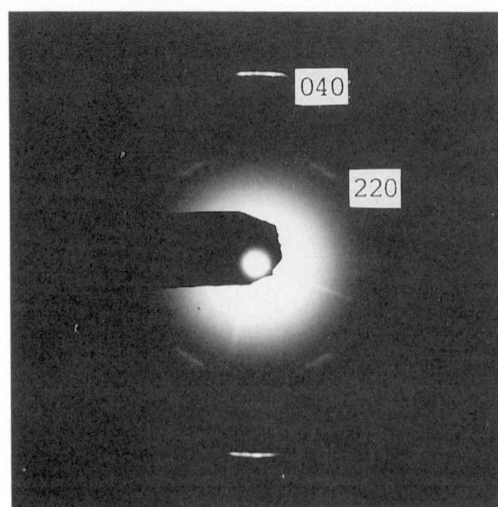
e



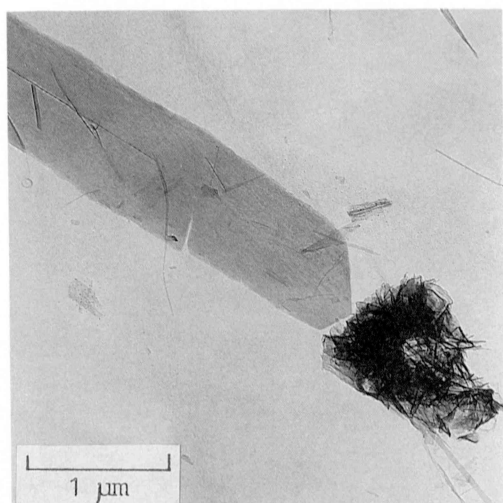
f



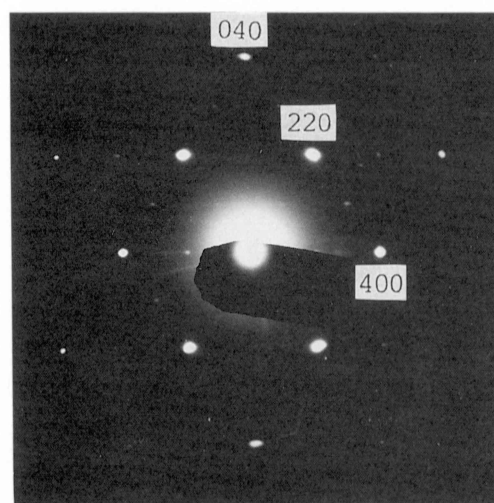
a



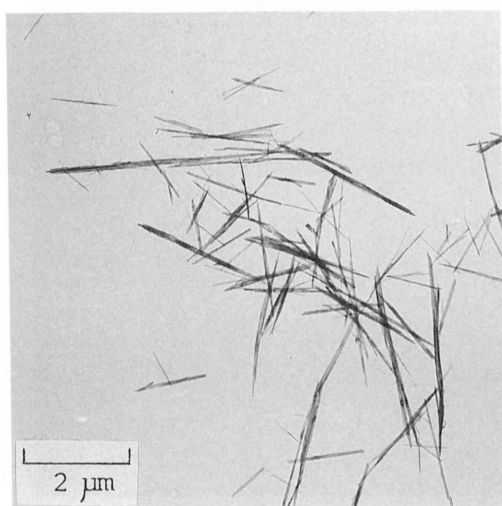
b



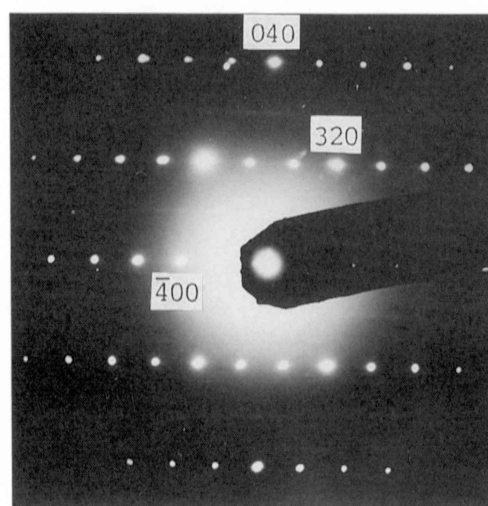
c



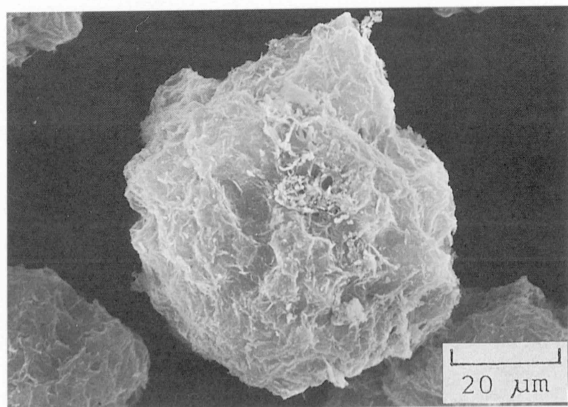
d



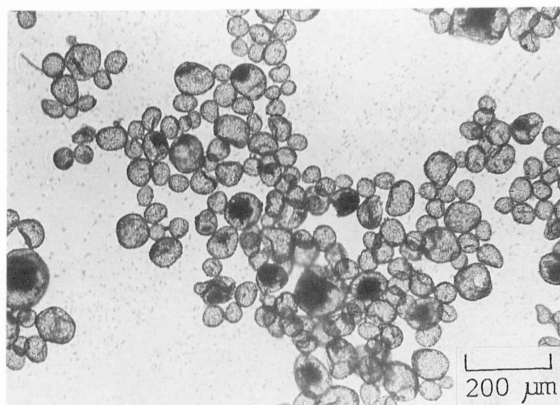
e



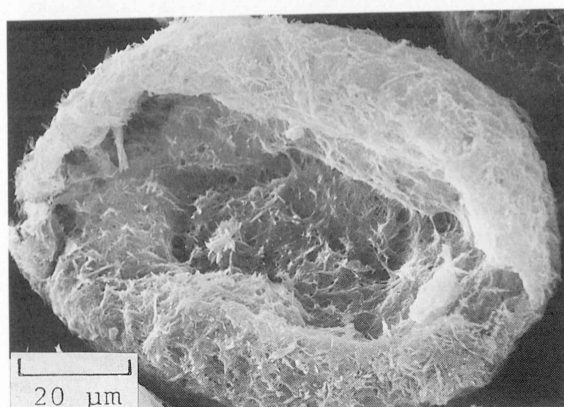
f



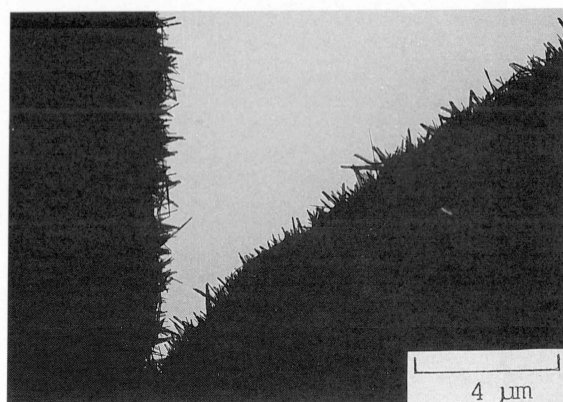
a



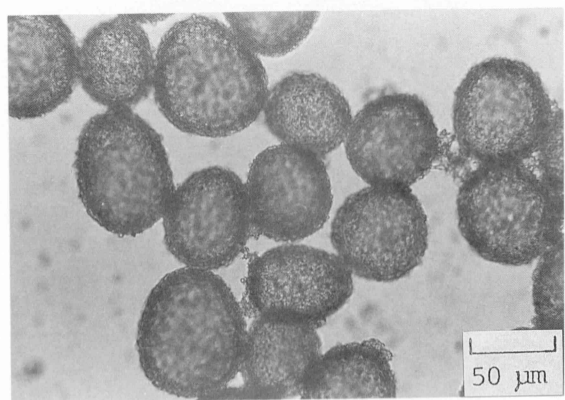
b



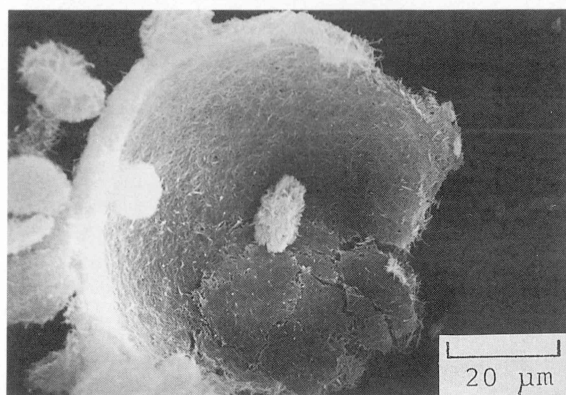
c



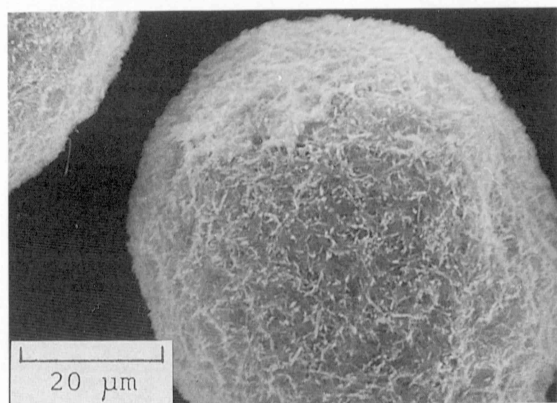
d



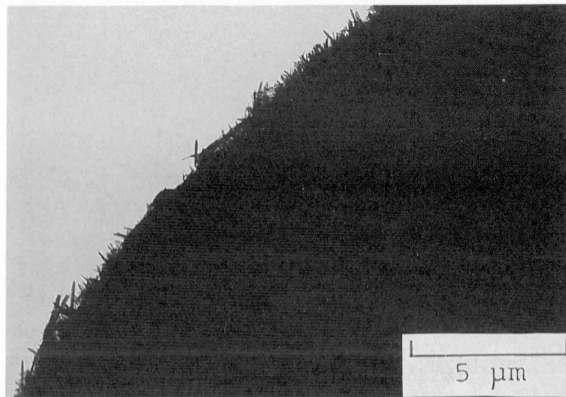
e



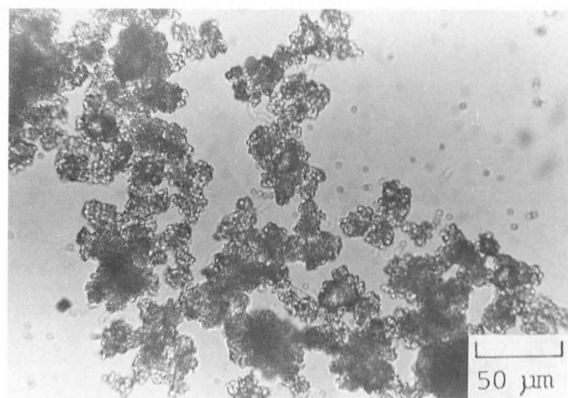
f



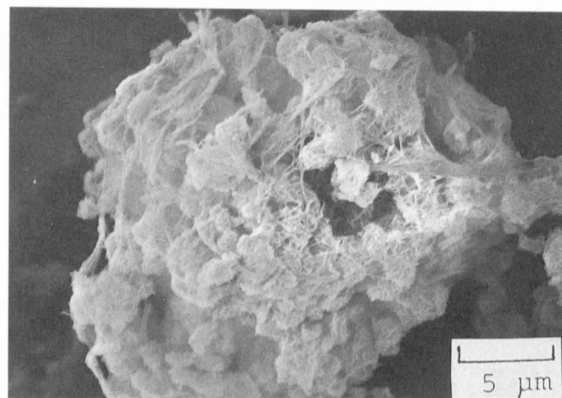
g



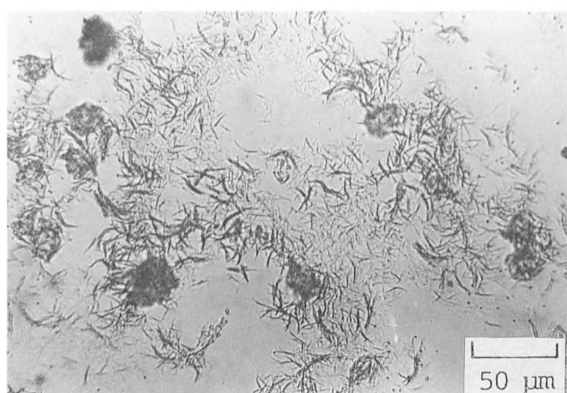
h



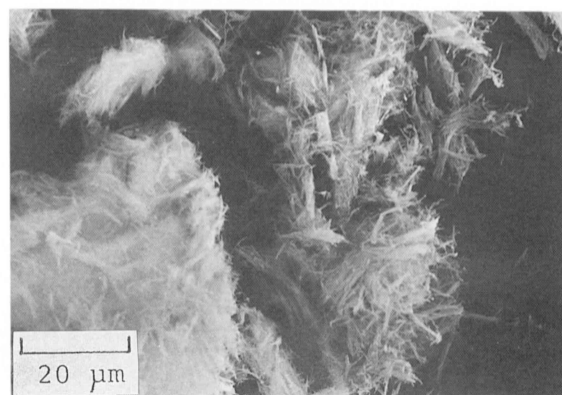
a



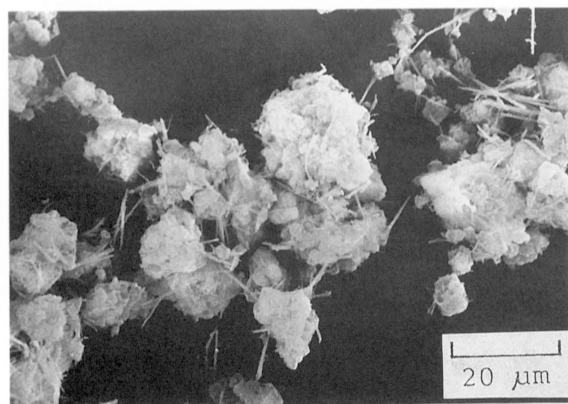
b



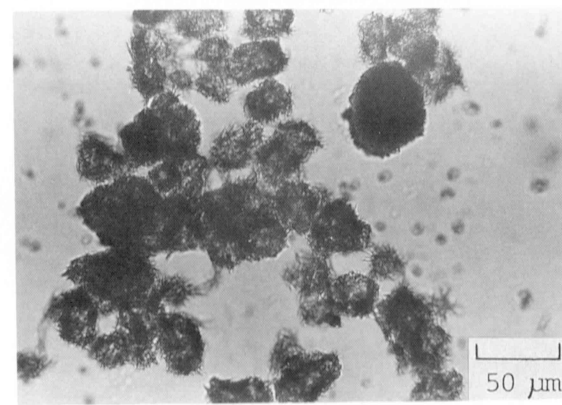
c



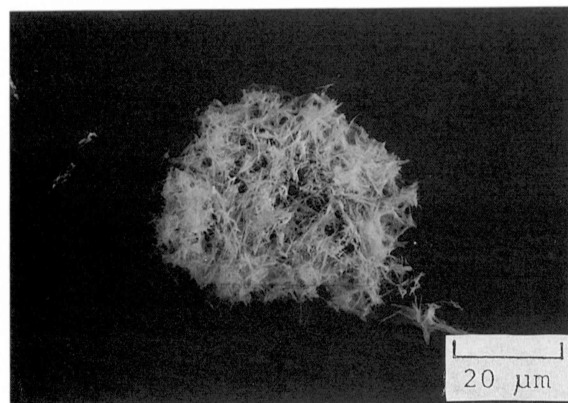
d



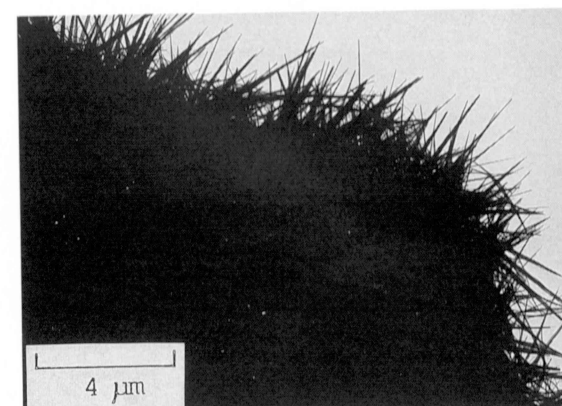
e



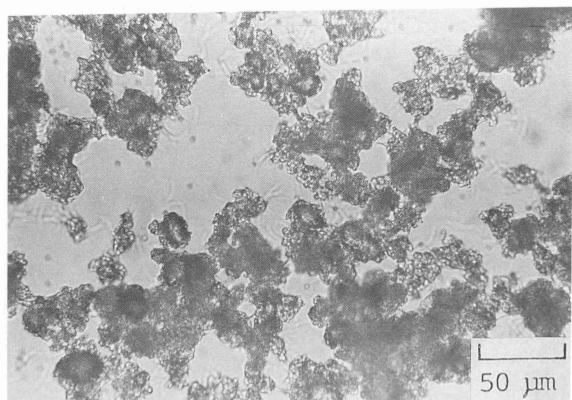
f



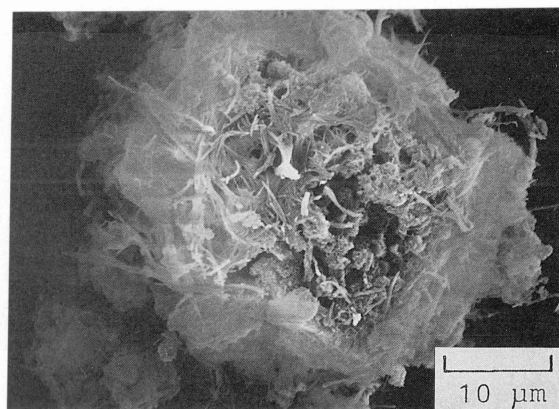
g



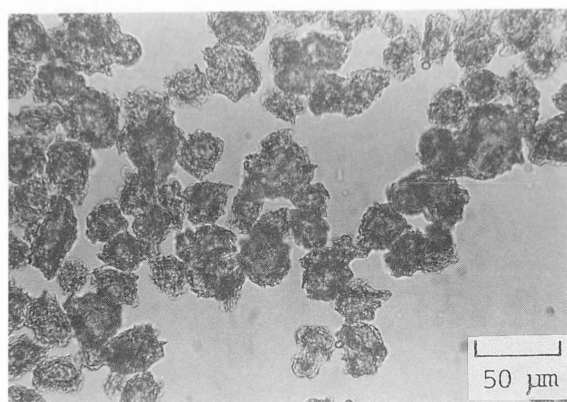
h



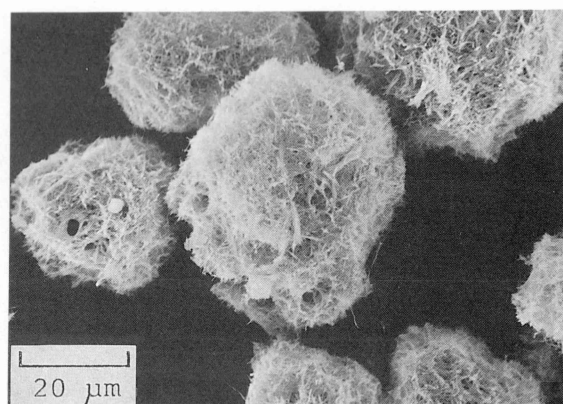
a



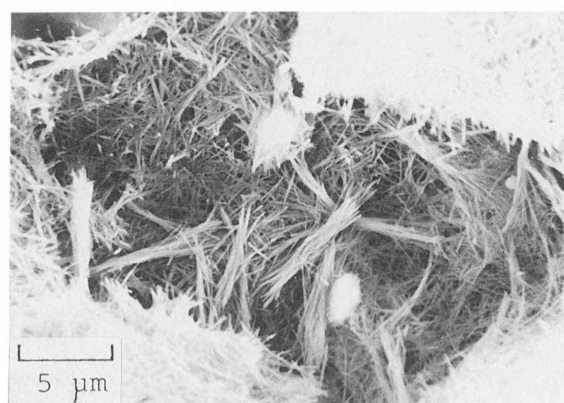
b



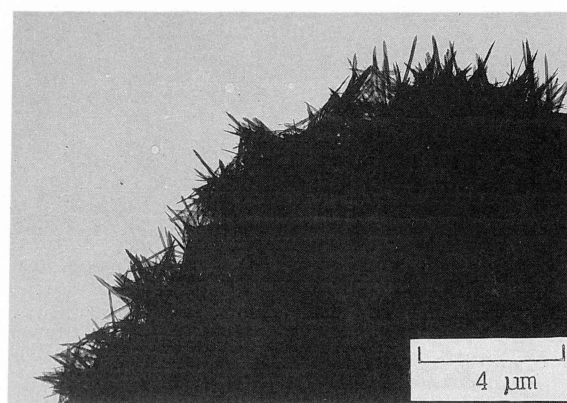
c



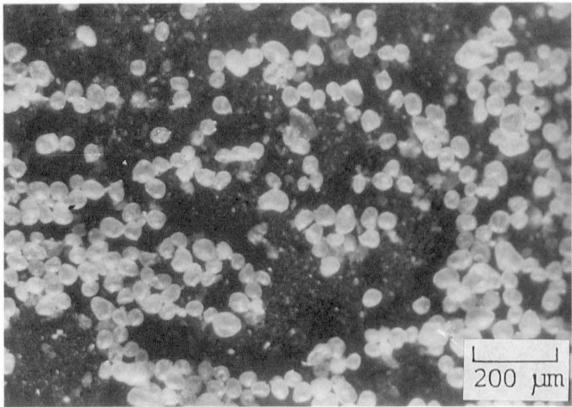
d



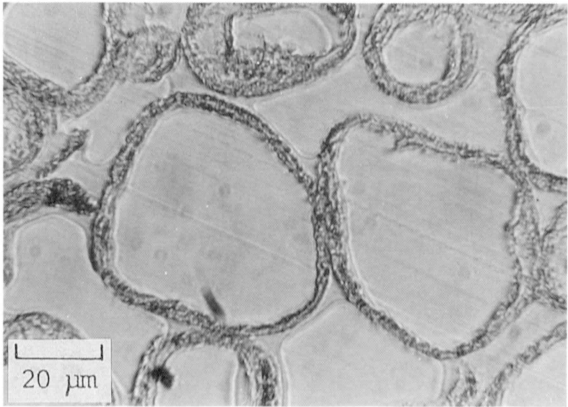
e



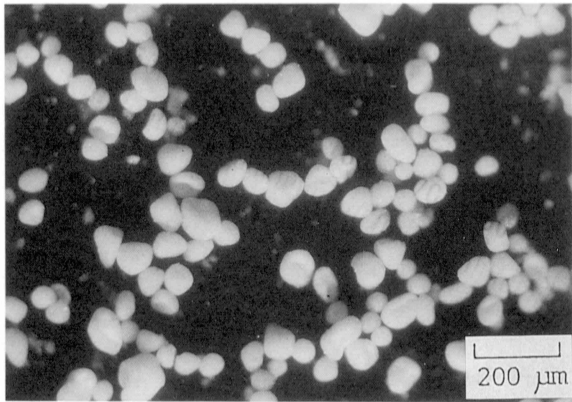
f



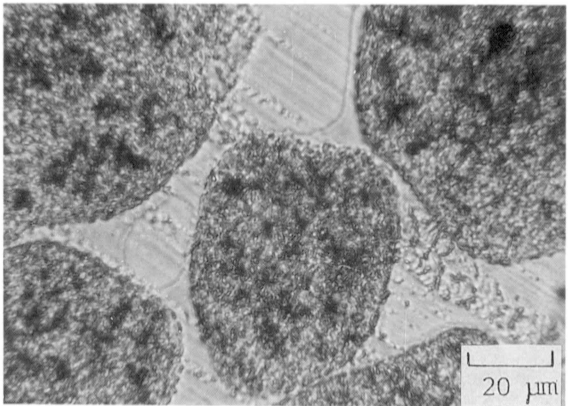
a



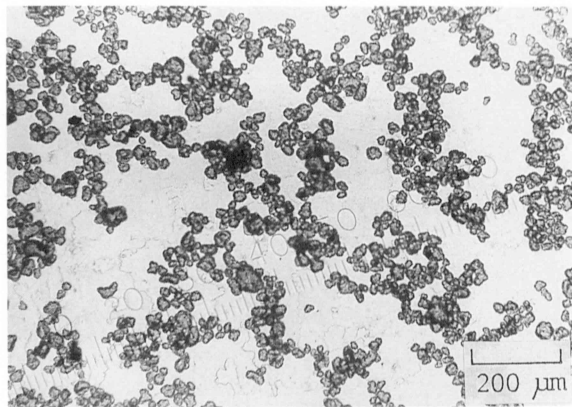
b



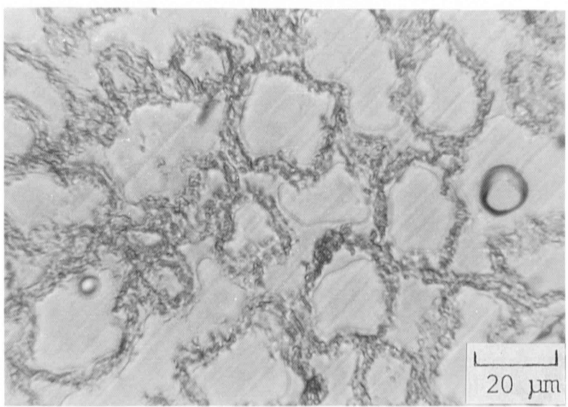
c



d



e



f